Insulin-like Growth Factor-1 Synergizes with IL-2 to Induce Homeostatic Proliferation of Regulatory T Cells

Melanie R. Shapiro,* Leeana D. Peters,* Matthew E. Brown,* Cecilia Cabello-Kindelan,† Amanda L. Posgai,* Allison L. Bayer,†,‡ and Todd M. Brusko*,§

IL-2 has been proposed to restore tolerance via regulatory T cell (Treg) expansion in autoimmunity, yet off-target effects necessitate identification of a combinatorial approach allowing for lower IL-2 dosing. We recently reported reduced levels of immunoregulatory insulin-like growth factor-1 (IGF1) during type 1 diabetes progression. Thus, we hypothesized that IGF1 would synergize with IL-2 to expand Tregs. We observed IGF1 receptor was elevated on murine memory and human naive Treg subsets. IL-2 and IGF1 promoted PI3K/Akt signaling in Tregs, inducing thymically-derived Treg expansion beyond either agent alone in NOD mice. Increased populations of murine Tregs of naive or memory, as well as CD5^{lo} polyclonal or CD5^{hi} likely self-reactive, status were also observed. Expansion was attributed to increased IL-2Rγ subunit expression on murine Tregs exposed to IL-2 and IGF1 as compared with IL-2 or IGF1 alone. Assessing translational capacity, incubation of naive human CD4^{+} T cells with IL-2 and IGF1 enhanced thymically-derived Treg proliferation in vitro, without the need for TCR ligation. We then demonstrated that IGF1 and IL-2 or IL-7, which is also IL-2Rγ-chain dependent, can be used to induce proliferation of genetically engineered naive human Tregs or T conventional cells, respectively. These data support the potential use of IGF1 in combination with common γ-chain cytokines to drive homeostatic T cell expansion, both in vitro and in vivo, for cellular therapeutics and ex vivo gene editing. ***The Journal of Immunology*****, 2023, 211: 1108–1122.**

Impairments in immunoregulation, including defective regulatory T cell (Treg) generation, as well as peripheral maintenance of phenotypically stable and functional Treg populations, have been suggested to contribute to the development of type 1 diabetes (T1D) and other autoimmune diseases (1, 2). Although human studies have largely shown that Treg numbers are not deficient in the peripheral blood of subjects with T1D or other organ-specific autoimmune conditions (1, 3–5), a dearth in the frequency of Tregs at the site of autoimmunity appears to be unique to T1D (6, 7). In contrast, defects in Treg suppressive function have been widely reported in multiple autoimmune conditions (1, 4), including T1D, wherein maintenance of Treg function is compromised in pancreatic draining lymph nodes of affected human organ donors (6). Efforts to specifically increase Tregs without influencing effector T cell numbers are therefore of great interest for T1D prevention.

Low-dose IL-2 has been proposed as a means to selectively enhance the proliferation and function of Tregs, which constitutively express CD25 (IL-2Rα), the α-chain subunit that creates the high-affinity trimeric IL-2R complex. This is in direct contrast with conventional CD4^{+} T cells (Tconvs), which must upregulate CD25 after activation (8). IL-2Rα pairs with the intermediate-affinity subunits IL-2Rβ and IL-2Rγ, which are less prone to change their expression with activation (9). Although the IL-2Rγ subunit, also known as the common γ-chain, can pair with several other cytokine receptor subunits to facilitate signaling by a wide variety of cytokines, including IL-7, IL-9, IL-15, and IL-21 in both Tregs and Tconvs (10), the restricted use of IL-2Rα in IL-2R belies the Treg-specific dependence on IL-2.

Impaired IL-2 signaling has been reported in Tregs of T1D subjects (11, 12). Moreover, decreased STAT5 phosphorylation downstream of IL-2R has been associated with T1D risk single-nucleotide polymorphisms in *CD25* and *PTPN2*, a phosphatase that inhibits JAK1 and JAK3 in the IL-2R pathway (12–14). Similarly, the NOD mouse carries a risk locus containing the *Il2* gene (15), which is thought to contribute to impaired Stat5 phosphorylation (16) and diminished survival of intraislet Tregs (17). These defects have been

*Department of Pathology, Immunology and Laboratory Medicine, College of Medicine, Diabetes Institute, University of Florida, Gainesville, FL; †Diabetes Research Institute, University of Miami Miller School of Medicine, Miami, FL; ‡Department of Microbiology and Immunology, University of Miami Miller School of Medicine, Miami, FL; and §Department of Pediatrics, College of Medicine, Diabetes Institute, University of Florida, Gainesville, FL

ORCIDs: 0000-0003-2090-0877 (M.R.S.); 0000-0002-7878-0014 (L.D.P.); 0000-0001-8230-5243 (M.E.B.); 0000-0002-9491-0958 (A.L.P.); 0000-0003-4778-0238 (A.L.B.); 0000-0003-2878-9296 (T.M.B.).

Received for publication August 30, 2022. Accepted for publication August 1, 2023.

This work was supported by grants from the National Institutes of Health (P01 AI042288 and UH3 DK122638 to T.M.B.; F31 DK117548 to M.R.S.; F31 DK129004 to L.D.P.); National Institute of Diabetes and Digestive and Kidney Diseases, National Institutes of Health (T32 DK108736 to M.R.S. and L.D.P.), Juvenile Diabetes Foundation Juvenile Diabetes Research Foundation (Postdoctoral Fellowship 3-PDF-2022-1137-A-N to M.R.S.), Diabetes Research Connection (project 45 to M.R.S.), The Leona M. and Harry B. Helmsley Charitable Trust (to T.M.B.), and the Diabetes Research Institute Foundation (to A.L.B.).

M.R.S. designed the studies, conducted experiments, acquired data, analyzed data, acquired funding, and wrote the manuscript; L.D.P. designed the studies, conducted experiments, acquired data, analyzed data, acquired funding, and edited the manuscript/edited the manuscript; M.E.B. designed the studies, conducted experiments, acquired data, analyzed data, and reviewed/edited the manuscript; C.C.-K. conducted experiments, acquired data, and reviewed/edited the manuscript; A.L.P. contributed to discussion and reviewed/edited the manuscript; A.L.B. designed the studies, analyzed data, acquired funding, and reviewed/edited the manuscript; T.M.B. conceptualized the project, designed studies, provided reagents, acquired funding, and reviewed/edited the manuscript.

Address correspondence and reprint requests to Dr. Todd M. Brusko, Department of Pathology, Immunology and Laboratory Medicine, College of Medicine, University of Florida, 1275 Center Drive, Biomedical Sciences Building J-589, Box 100275, Gainesville, FL 32610. E-mail address: tbrusko@ufl.edu

The online version of this article contains supplemental material.

Abbreviations used in this article: AF, Alexa Fluor; BV, Brilliant Violet; CAR, chimeric Ag receptor; cRPMI, complete RPMI; DI, division index; DN, double-negative; DP, double-positive; GAD65, glutamic acid decarboxylase 65; gMFI, geometric mean fluorescence intensity; IAC, IL-2 Ab complex; IGF1, insulin-like growth factor-1; IGF1R, insulin-like growth factor-1 receptor; pLN, pancreatic lymph node; pTreg, peripherally-induced regulatory T cell; rh, recombinant human; SP, single-positive; STZ, streptozotocin; Tconv, conventional CD4^{+} T cell; T1D, type 1 diabetes; Treg, regulatory T cell; tTreg, thymically-derived regulatory T cell; UF, University of Florida;

This article is distributed under The American Association of Immunologists, Inc., Reuse Terms and Conditions for Author Choice articles.

Copyright © 2023 by The American Association of Immunologists, Inc. 0022-1767/23/$37.50

corrected with low-dose IL-2 therapy in both mice (17) and humans (18), with success in improving IL-2 targeting to murine Tregs via the addition of an IL-2–specific mAb (IL-2 Ab complex [IAC]) enhancing IL-2 half-life and blocking interaction with the intermediate-affinity IL-2R complex (19). Despite such improvements to IL-2 delivery, inflammatory cell subsets expressing CD25, such as memory T cells and NK cells, have been reported to expand alongside Tregs (18–20). This highlights the need to identify combination therapies that synergize with IL-2, allowing for efficacy with lower IL-2 doses and avoidance of off-target effects.

Insulin-like growth factor-1 (IGF1) is an immunoregulatory hormone (21) that we recently showed to be significantly reduced in serum from individuals during pre-T1D and after T1D diagnosis (22), potentially contributing to the progression of autoimmunity (23). Low peripheral IGF1 levels have been previously implicated in the pathogenesis of autoimmune disorders, including rheumatoid arthritis (free and total IGF1) (24), Crohn's disease (total IGF1) (25, 26), and T1D (total IGF1) (22). IGF1 has previously been shown to promote the in vitro proliferation of sorted human Tregs (27). In addition, IGF1 treatment inhibited T1D development in the NOD and streptozotocin-induced models, with the latter ascribed to increased Treg proliferation in peripheral blood, leading to elevated numbers of Tregs in the pancreas (27). Likewise, the development of murine experimental autoimmune encephalitis (27) and allergic contact dermatitis (28) were inhibited by IGF1, with elevated numbers of $Foxp3^+$ Tregs observed at the site of autoimmunity, as a direct consequence of Treg-specific IGF1:IGF1 receptor (IGF1R) signaling. These studies suggest that IGF1 may induce immunoregulation through the preferential induction of Treg proliferation as compared with Tconvs.

Despite this propensity for IGF1 to impact Tregs, the mechanisms by which this growth factor engages the IGF1R and induces downstream PI3K/Akt signaling (29) and proliferation of Tregs from bulk $CD4^+$ T cell populations remains unclear. In addition, IL-2 and IGF1 combination treatment has yet to be evaluated as a synergistic approach toward promoting Treg expansion. Therefore, we hypothesized that IGF1 may augment the extent to which IL-2 preferentially induces Treg expansion. In this study, we demonstrate IL-2 and IGF1 synergism in murine and human Tregs while providing mechanistic insights and establishing evidence for the feasibility of in vivo therapeutic and in vitro laboratory applications of this combinatorial treatment.

Materials and Methods

Murine IGF1R staining

Spleen and thymus of 6-wk-old NOD.Foxp3-GFP/cre mice (Stock No. 008694; Jackson Laboratory) were processed using frosted glass slides and passed through a 40-μm filter to create single-cell suspensions. RBCs were lysed with ammonium-chloride-potassium buffer before staining for flow cytometry. Samples were stained with Fixable Live/Dead Near IR (Invitrogen) and washed once with stain buffer (PBS + 2% FBS + 0.05% NaN_3), and Fc receptors were blocked with anti-CD16/32 for 5 min at 4°C (Clone 2.4G2; BD Biosciences). Samples were stained for 30 min at 4°C with the following anti-mouse Abs: CD3e-Brilliant Violet (BV) 605 (145-2C11; BioLegend), CD4-PerCP/Cy5.5 (RM4-5; Thermo Fisher Scientific), CD8a-BV711 (53-6.7; BioLegend), CD44-PE-Cy7 (IM7; BioLegend), CD62L-allophycocyanin (MEL-14; BioLegend), and CD221-PE (3B7; Santa Cruz Biotechnology). Samples were washed once with stain buffer before data acquisition on an LSRFortessa (BD Biosciences) and analysis with FlowJo (v10.6.1; Tree Star) according to gating schemes shown in Supplemental Figure 1.

Murine IGF1R signaling

Single-cell suspensions of splenocytes were generated from 16- to 22-wk-old prediabetic NOD/ShiLtJ mice (Stock No. 001976, Jackson Laboratory), followed by RBC lysis. Cells were resuspended at 10^6/ml in complete RPMI (cRPMI) 1640 without L-glutamine (Corning; cRPMI [supplemented with 2 mM GlutaMAX (Life Technologies), 100 IU and 100 μg/ml each of penicillin-streptomycin solution (Corning), 1 mM sodium pyruvate (Corning), 0.1 mM nonessential amino acids (Life Technologies), 10 mM HEPES (Life Technologies), 10% FBS (GenClone), and 0.0004% 2-ME (Sigma-Aldrich)]) and treated with 10 IU/ml recombinant human (rh) IL-2 (Teceleukin) and/or 100 ng/ml rhIGF1 (BioVision) for 15 or 60 min at 37°C. Samples were fixed with an equal volume of Cytofix fixation buffer (BD Biosciences) for 10 min at 37°C. Live/Dead fixable near-IR dead cell stain kit (Invitrogen) was applied according to the manufacturer's instructions for dead cell exclusion. Cells were washed once with stain buffer, permeabilized with Phosflow perm buffer III (BD Biosciences) for 30 min at 4°C, washed twice with stain buffer, and then incubated with anti-CD16/32 (Clone 2.4G2; BD Biosciences) for 5 min at 23°C. Samples were stained with the following fluorescently labeled anti-mouse Abs at 23°C for 45 min: CD3-PerCP-Cy5.5 (17A2), CD4-BV711 (RM4-5), CD44-PE-Cy7 (IM7), Helios-Pacific Blue (22F6) (BioLegend), Foxp3-Alexa Fluor (AF)-AF488 (FJK-16s; eBioscience), pS6 Ser235/236-AF647 (D57.2.2E; Cell Signaling Technology), and p-STAT5 Tyr694-PE (47/STAT5; BD Biosciences). Samples were washed once with stain buffer before data acquisition on an LSRFortessa (BD Biosciences) and analysis with FlowJo software (v10.6.1; Tree Star).

Murine IGF1 + low-dose IL-2 treatment

Prediabetic 12-wk-old female NOD/ShiLtJ mice were treated with IAC (5 μg anti–IL-2 [JES6-1A12; eBioscience] + 1 μg recombinant mouse IL-2) injected i.p. every other day for a week as we previously reported (30), 10 μg rhIGF1 injected s.c. twice a day for 3 wk (31), IAC + IGF1 in combination, or vehicle control (PBS). Peripheral blood was collected before treatment and on a weekly basis during the treatment regimen for flow cytometric analysis. RBCs were lysed before staining with Live/Dead fixable near-IR dead cell stain kit (Invitrogen). Cells were stained with the following Abs: CD19-allophycocyanin-Cy7 (1D3; BD Biosciences), Ly6G-allophycocyanin-Cy7 (1A8; BD Biosciences), CD122-Biotin (TM-β1; BD Biosciences), CD45-BV510 (30-F11; BD Biosciences), CD5-BV650 (53-7.3; BD Biosciences), CD4-PE-Cy7 (RM4-5; BioLegend), CD8-AF700 (53-6.7; BioLegend), CD25-PE-CF594 (PC61; BD Biosciences), CD335-PE (29A1.4; BD Biosciences), and cKIT (CD117)-Brilliant Blue-700 (2B8; BD Biosciences), CD44-BV605 (IM7; BD Biosciences), before a wash with stain buffer and application of a Streptavidin-BV711 (BD Biosciences) conjugate. Samples were fixed and permeabilized with Foxp3 transcription factor staining buffer set according to the manufacturer's protocol (ThermoFisher) before staining with anti-mouse Helios-allophycocyanin (22F6; BioLegend), Foxp3-eFluor 450 (FJK-16s; ThermoFisher), Eomes-AF488 (Dan11ma; ThermoFisher), and Ki67-BV786 (B56; BD Biosciences). Peripheral lymphoid organs, including spleen, lymph nodes, and thymi, were collected and processed to single-cell suspensions at the end of the treatment regimen for flow cytometric analysis. RBCs were lysed before staining with Live/Dead fixable near-IR dead cell stain kit (Invitrogen). Cells were stained with the following Abs: CD19-allophycocyanin-Cy7 (1D3; BD Biosciences), CD45-BV510 (30-F11; BD Biosciences), CD3-AF700 (17A2; BioLegend), CD4-PE-Cy7 (RM4-5; BioLegend), CD8-PerCP-Cy5.5 (53-6.7; BioLegend), CD44-PE-CF594 (IM7; BD Biosciences), CD127-BV786 (SB/199; BD Biosciences), CD39-PE (24DMS1; eBioscience), CD73-BV605 (TY/11.8; BioLegend), CD25-BV711 (PC61; BD Biosciences), CD122-Biotin (TM-β1; BD Biosciences), before a wash with stain buffer and application of a Streptavidin-BV650 (BD Biosciences) conjugate. Samples were fixed and permeabilized with Foxp3 transcription factor staining buffer set according to the manufacturer's protocol (ThermoFisher) before staining with anti-mouse Helios-allophycocyanin (22F6; BioLegend), Foxp3-eFluor 450 (FJK-16s; ThermoFisher), and Ki67-FITC (B56; BD Biosciences). Data were acquired on an LSRII (BD Biosciences) and analyzed with KALUZA software (v2.1).

Murine IL-2R subunit and IGF1R cross-regulation by IGF1 and IL-2

Single-cell suspensions of splenocytes were generated from 6- to 7-wk-old prediabetic NOD.Foxp3-GFP/cre mice (Stock No. 008694; Jackson Laboratory), followed by RBC lysis. Cells were resuspended at 10^6/ml in cRPMI and treated with 10 IU/ml rhIL-2 (Teceleukin) and/or 100 ng/ml rhIGF1 (BioVision) for 2 d at 37°C. Live/Dead fixable near-IR dead cell stain kit (Invitrogen) was applied according to manufacturer's instructions for dead cell exclusion. Cells were washed once with stain buffer and then incubated with anti-CD16/32 (Clone 2.4G2; BD Biosciences) for 5 min at 4°C. Samples were stained with the following fluorescently labeled anti-mouse Abs at 4°C for 30 min: CD4-PerCP-Cy5.5 (RM4-5; eBioscience), CD62L-BV510 (MEL-14; BioLegend), CD44-PE-Cy7 (IM7; BioLegend), CD221-PE (3B7; Santa Cruz Biotechnology), CD25-AF700 (PC61), CD122-PE-Dazzle594 (TM-β1), and CD132-allophycocyanin (TUGm2) (BioLegend). Samples were fixed and permeabilized with Foxp3 transcription factor staining buffer set according to the manufacturer's protocol (eBioscience) before staining

for 45 min at 23°C with anti-mouse Foxp3-AF488 (FJK-16s; eBioscience) and Helios-Pacific Blue (22F6; BioLegend). Samples were washed once with stain buffer before data acquisition on a Cytek Aurora 5L (16UV-16V-14B-10YG-8R) spectral flow cytometer and analysis with FlowJo software (v10.6.1; Tree Star).

Human subject enrollment

Study subjects were recruited from the Children with Diabetes–sponsored Friends for Life Conference held annually in Orlando, FL; the general population; or outpatient clinics at the University of Florida (UF; Gainesville, FL); Nemours Children's Hospital (Orlando, FL); and Emory University (Atlanta, GA). After providing written informed consent, peripheral blood samples were collected into the UF Diabetes Institute Study Bank from nonfasted subjects by venipuncture in heparin-coated vacutainer tubes (BD Biosciences) in accordance with institutional review board–approved protocols. Leukapheresis-processed blood of healthy donors was also purchased from LifeSouth Community Blood Centers (Gainesville, FL). Samples were selected from non-T1D subjects, as well as age- and sex-matched T1D patients, for fresh whole blood staining, with detailed deidentified demographic information presented in Table I. For the remainder of experiments performed, peripheral blood samples were selected from healthy subjects (Table II).

Human whole blood flow cytometry

To determine IGF1R expression, we stained 200 μl of whole blood with the following fluorescently labeled anti-human Abs for 30 min at 23°C in the dark: CD25-AF488 (BC96), CD127-BV421 (A019D5), CD197-AF647 (G043H7), CD45RA-PerCP-Cy5.5 (HI100), CD3-allophycocyanin-Fire750 (SK7), CD221-PE (1H7) (BioLegend), CD4-PE-Cy7 (RPA-T4; eBioscience). RBCs were lysed for 5 min at 23°C with 1-step Fix/Lyse Solution (eBioscience), followed by three washes with stain buffer. Data were acquired on an LSRFortessa (BD Biosciences) and analyzed with FlowJo software (v10.6.1; Tree Star) according to gating schemes shown in Supplemental Figure 2.

Human IGF1R signaling

Whole blood was processed to PBMCs via density gradient centrifugation. PBMCs were incubated overnight at 10^6 cells/ml with 2 μg/ml ultra-low endotoxin, azide-free purified anti-human CD3 (OKT3; BioLegend) and 1 μg/ml no azide/low endotoxin-purified anti-human CD28 (CD28.2; BD Biosciences) in cRPMI. The following day, samples were stimulated with 100 ng/ml rhIGF1 (BioVision) for 15 or 30 min at 37°C and then immediately fixed with an equal volume of Cytofix fixation buffer (BD Biosciences) for 10 min at 37°C. Live/Dead fixable near-IR dead cell stain kit (Invitrogen) was applied according to manufacturer's instructions for dead cell exclusion. Cells were washed once with stain buffer, permeabilized with Phosflow perm buffer III (BD Biosciences) for 30 min on ice, washed twice with stain buffer, and then incubated with human TruStain FcX (BioLegend) for 5 min at 23°C. Samples were stained with the following fluorescently labeled anti-human Abs at 23°C for 45 min: CD3-PerCP-Cy5.5 (UCHT1), CD45RA-BV711 (HI100), FOXP3-AF488 (206D), FOXP3-AF488 (259D), Helios-Pacific Blue (22F6) (BioLegend), CD4-PE-Cy7 (RPA-T4; eBioscience), pS6 Ser235/236-AF647 (D57.2.2E), and pAkt Ser473-PE (D9E) (Cell Signaling Technology). Samples were washed once with stain buffer before data acquisition on an LSRFortessa (BD Biosciences) and analysis with FlowJo software (v10.6.1; Tree Star).

In vitro homeostatic proliferation

Naive $CD4^+$ T cells were isolated by either density gradient centrifugation of whole blood followed by EasySep human naive $CD4^+$ T cell enrichment kit (19155; STEMCELL Technologies) or by RosetteSep human $CD4^+$ T cell enrichment (STEMCELL Technologies) of whole blood followed by human CD45RO microbead depletion (Miltenyi Biotec). Enriched cells were stained with Cell Proliferation Dye eFluor670 (Thermo Fisher) according to the manufacturer's instructions. Naive $CD4^+$ T cells were plated at 10^6 cells/ml in cRPMI with 20 IU/ml rhIL-2 (Teceleukin) and 100 ng/ml rhIGF1 (BioVision). Cytokine and/or growth factor was replenished on days 3 and 7, assuming consumption, and intracellular flow cytometry was performed on days 9–11. Live/Dead fixable near-IR dead cell stain kit (Invitrogen) was applied according to the manufacturer's instructions for dead cell exclusion. Cells were washed once with stain buffer and incubated with human TruStain FcX (BioLegend) for 5 min at 4°C. Samples were stained with the following fluorescently labeled anti-human Abs for 30 min at 4°C: CD4-PerCP-Cy5.5 (RPA-T4), CD45RA-BV711 (HI100), and CD221-PE (1H7) (BioLegend) before fixation and permeabilization with FOXP3 transcription factor staining buffer set according to the manufacturer's protocol (eBioscience). Intracellular staining was performed with the following fluorescently labeled anti-human Abs for 30 min at 23°C: FOXP3-AF488 (206D), FOXP3-AF488 (259D), and Helios-Pacific Blue (22F6) (BioLegend). Data were acquired on an LSRFortessa (BD Biosciences) and analyzed with FlowJo software (v10.6.1; Tree Star).

Human T cell transduction

Naive $CD4^+$ T cells were isolated by density gradient centrifugation of PBMCs from whole blood followed by use of Naive $CD4^+$ T cell Isolation Kit II (Miltenyi Biotec). Cells were stained with Cell Proliferation Dye eFluor670 (eBioscience) and cultured at 10^6/ml with 20 IU/ml rhIL-2 (Teceleukin), 10 ng/ml rhIL-7 (BD Biosciences), and/or 100 ng/ml rhIGF1 (BioVision) for 7 d before transduction. Cells were transduced using 8 μg/ml protamine sulfate (Sigma-Aldrich) and 3 transduction units/cell lentiviral vector containing R164, a TCR recognizing T1D-relevant epitope glutamic acid decarboxylase 65 (GAD65) 555–567 in the context of HLA-DRB1*04:01 (32). Lentiviral vector composition (33) and production (34) were as previously described. Cells were spinoculated by centrifugation at 1000 × *g* for 30 min at 32°C (34), and IL-2, IL-7, and/or IGF1 were added assuming consumption on days 3, 7, and 10. Cells were harvested on day 14, and Live/Dead fixable near-IR dead cell stain kit (Invitrogen) was applied according to the manufacturer's instructions for dead cell exclusion. Cells were washed once with stain buffer, then incubated with human TruStain FcX (BioLegend) for 5 min at 4°C. Samples were stained with the following fluorescently labeled anti-human Abs at 4°C for 30 min: TCR Vβ5.1-PE (IMMU 157; Beckman Coulter), CD45RA-BV711 (HI100), and CD197-PE-Cy7 (G043H7) (BioLegend). Samples were fixed and permeabilized with Foxp3 transcription factor staining buffer set according to the manufacturer's protocol (eBioscience) before staining for 30 min at 23°C with anti-human FOXP3-AF488 (206D), FOXP3-AF488 (259D), and Helios-Pacific Blue (22F6) (BioLegend). Samples were washed once with stain buffer before data acquisition on an LSRFortessa (BD Biosciences) and analysis with FlowJo software (v10.6.1; Tree Star).

Statistics

Analyses were performed using GraphPad Prism software version 7.0. Data are presented as mean ± SD, and all tests were two-sided unless otherwise specified. Murine IGF1R expression was compared between cell subsets using repeated measures one-way ANOVA with Bonferroni's multiple comparisons test. IGF1R signaling was compared over the time course between treatment groups using a nonlinear regression with extra-sum-of-squares F test. One-way ANOVA with Dunnett's or Tukey's multiple comparisons tests was used to assess outcomes of in vivo IL-2 + IGF1 treatment when comparing all treatment groups with each other or only with PBS control, respectively. IL-2R subunit and IGF1R expression were compared between treatment conditions using repeated-measures one-way ANOVA with Tukey's multiple comparisons test. Friedman test or Kruskal–Wallis test with Dunn's multiple comparisons test were used to compare IGF1R expression on $CD4^+$ T cell subsets within human subjects or between T1D and non-T1D subjects, respectively. Associations between IGF1R levels and subject age were assessed via Spearman correlation. Human in vitro proliferation and lentiviral transduction were compared between experimental conditions via Wilcoxon test or paired *t* test, depending upon whether the data were normally distributed, as assessed by Shapiro–Wilk test. The p values <0.05 were considered significant.

Study approval

All procedures with human samples were approved by the institutional review board at each institution and conducted in accordance with the Declaration of Helsinki. Written informed consent was obtained from participants (or their legal guardian in the case of minors) before enrollment. NOD/ShiLtJ and NOD.Foxp3-GFP/cre mice were bred at the UF for in vitro experiments or purchased from Jax by the University of Miami for in vivo experiments and housed in specific pathogen-free facilities, with food and water available ad libitum. All murine studies were conducted in accordance with protocols approved by the UF or University of Miami Institutional Animal Care and Use Committee and in accordance with the National Institutes of Health *Guide for the Care and Use of Animals*.

Results

IGF1R expression during T cell development and activation in NOD mice

We hypothesized that IGF1 may preferentially induce Treg proliferation because of increased IGF1R expression on this subset as compared with Tconvs. Thus, we measured IGF1R expression by flow cytometry on NOD.Foxp3-GFP thymocyte and splenocyte populations through the stages of central development and peripheral activation,

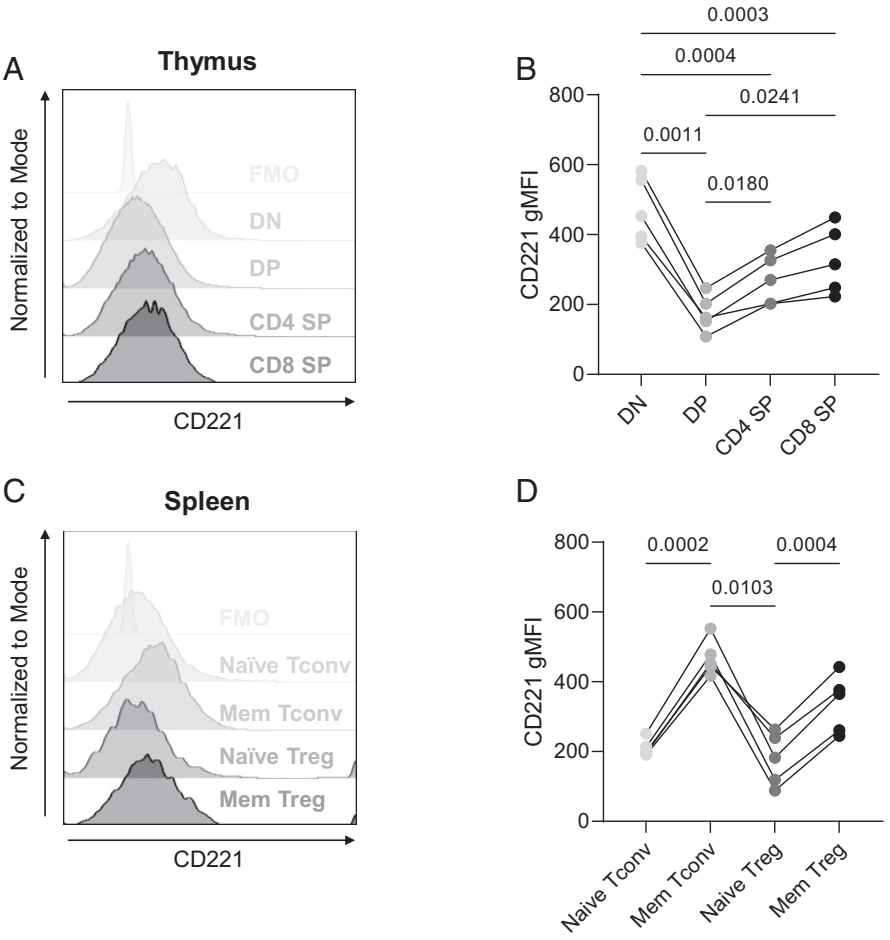

FIGURE 1. Murine IGF1R expression across the maturation stages of Tconvs and Tregs. Thymus and spleen of prediabetic NOD.Foxp3-GFP mice were stained for IGF1R and differentiation of $CD4^+$ and $CD8^+$ naive and memory T cells via flow cytometry. (**A**) Representative histograms of IGF1R/CD221 expression on fluorescence-minus-one (FMO) negative control, $CD4^-CD8^-$ DN, $CD4^+CD8^+$ DP, $CD4^+CD8^-$ SP (CD4 SP), and $CD4^-CD8^+$ (CD8 SP) thymocytes. (**B**) gMFI of IGF1R at various stages of thymocyte development. (**C**) Representative histograms of IGF1R expression on FMO negative control, naive ($CD62L^+CD44^{lo}$) and memory ($CD62L^-CD44^{hi}$) Tconv ($CD4^+Foxp3^-$) and Treg ($CD4^+Foxp3^+$) populations in spleen. (**D**) gMFI of IGF1R on $CD4^+$ T cell subpopulations. Repeated-measures one-way ANOVA with Bonferroni's multiple comparisons test. $n = 5$ mice.

respectively. IGF1R expression was highest on $CD4^-CD8^-$ double-negative (DN) thymocytes (geometric mean fluorescence intensity [gMFI] of 472.20 ± 93.30) as compared with later developmental stages ($CD4^+CD8^+$ double-positive [DP], 174.20 ± 52.67; $CD4^+CD8^-$ single-positive (SP), 271.2 ± 69.76; $CD4^-CD8^+$ SP, 327.20 ± 96.90; Fig. 1A, 1B, Supplemental Fig. 1A), in agreement with a previous study showing that human DN thymocytes express approximately three times more surface IGF1R protein than $CD4^+CD8^+$ DP thymocytes (35). IGF1R expression rebounded partially in $CD4^+CD8^-$ and $CD4^-CD8^+$ SP thymocytes (Fig. 1A, 1B, Supplemental Fig. 1A), remaining lower than in DN thymocytes. In the periphery, splenic $CD4^+Foxp3^-CD44^{hi}CD62L^-$ memory Tconvs showed significantly higher levels of IGF1R (468.80 ± 51.37) than $CD4^+Foxp3^-CD44^{lo}CD62L^+$ naive Tconvs (209.60 ± 24.63; Fig. 1C, 1D, Supplemental Fig. 1B), as previously reported in BALB/c mice (36). This expression pattern was replicated upon comparing naive and memory $CD4^+Foxp3^+$ Tregs (178.22 ± 75.04 versus 337.80 ± 83.02; Fig. 1C, 1D, Supplemental Fig. 1B), suggesting that differential IGF1R levels may partially account for IGF1-mediated T cell regulation via impacts on memory Tregs in mice.

IGF1 and IL-2 synergize in vitro to preferentially induce IGF1R signaling in NOD Tregs

IGF1R signaling was assessed in splenocytes from NOD mice via Phosflow staining to determine whether IGF1R protein expression directly correlated with the magnitude of IGF1R signaling. Modest IGF1-mediated induction of pS6 (Ser235/236), a measure of PI3K/Akt signaling downstream of IGF1R (37), was observed in $CD4^+Foxp3^+Helios^+$ Tregs (1.38-fold increase at 15 and 60 min posttreatment; Fig. 2A–C, Supplemental Fig. 1C). Thus, we hypothesized that IGF1 could potentially synergize with other inducers of the PI3K/Akt pathway, such as cytokines, to augment Treg IGF1R signaling. In particular, IL-2 has previously been shown to preferentially induce the proliferation of Tregs (38). Therefore, we treated murine splenocytes with low-dose IL-2 in combination with IGF1 to test whether IGF1 could further enhance Treg PI3K/Akt signaling. Indeed, the combination enhanced Treg-specific pS6 in a synergistic manner (2.15-fold increase at 15 and 60 min) beyond that of either agent alone (IGF1: 1.38-fold increase at 15 and 60 min; IL-2: 1.22- and 1.49-fold increase at 15 and 60 min posttreatment, respectively; Fig. 2A–C). Importantly, the synergy was specific to the Treg compartment, because the combination treatment did not significantly increase the percentage of $pS6^+$ naive or memory Tconvs (Fig. 2A, 2B). In contrast with the PI3K/Akt pathway, IL-2R signaling, as demonstrated by pstat5 (Tyr694) induction by IL-2, was unaffected by the addition of IGF1 (Fig. 2D–F). Together, these data imply that IGF1 and IL-2 are capable of synergizing to promote murine Treg-specific IGF1R signaling and thereby may promote downstream effects of PI3K/Akt signaling such as cellular proliferation and survival.

IGF1 and IL-2 synergize in vivo to promote Treg proliferation

To assess whether our in vitro observation of IGF1 and IL-2 treatment supporting Treg-specific IGF1R signaling would translate to in vivo Treg expansion, we treated prediabetic NOD mice with 10 μg rhIGF1 twice daily for 3 wk (31) and/or IAC, a method commonly used to extend the half-life of low-dose IL-2, every other day for 1 wk (30) (Fig. 3A). We examined populations known to proliferate in response to IL-2 treatment, including $CD8^+$ T cells, $CD4^+Foxp3^-$ Tconvs, $CD4^+Foxp3^+$ Tregs, and NK cells (18, 19), in the peripheral blood of treated mice. Importantly, the combination of IGF1 plus IAC resulted in a

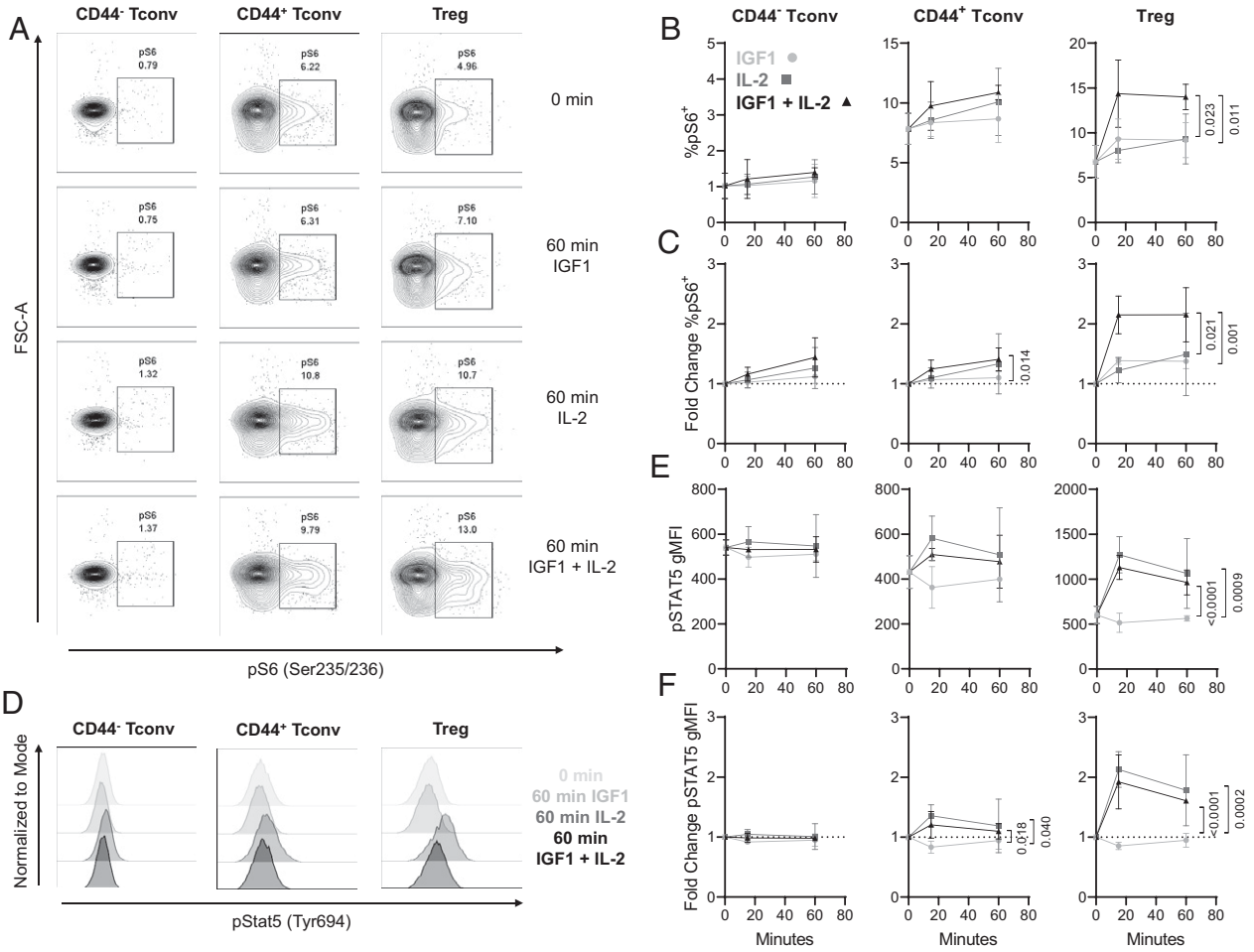

FIGURE 2. IGF1 synergizes with IL-2 to promote PI3K/Akt signaling specifically in Tregs of NOD mice. Splenocytes of prediabetic mice (16–22 wk old) were stimulated with IGF1 (100 ng/ml), IL-2 (10 IU/ml), or IGF1 + IL-2 for 15 or 60 min before Phosflow staining. (**A**) Representative contour plots of pS6 (Ser235/236) induction in CD44$^-$ Tconvs (CD4$^+$Foxp3$^-$Helios$^-$), CD44$^+$ Tconvs, and Tregs (CD4$^+$Foxp3$^+$Helios$^+$). (**B**) % pS6$^+$ cells over the time course. (**C**) Data in (B) were normalized by % pS6$^+$ cells without treatment per mouse to calculate fold change. (**D**) Representative histograms of pStat5 (Tyr694) induction in CD44$^-$ Tconvs, CD44$^+$ Tconvs, and Tregs without treatment or treated for 60 min with 100 ng/ml rhIGF1, 10 IU/ml rhIL-2, or rhIL-2 + rhIGF1. (**E**) gMFI of pstat5 in each cell population over the time course. (**F**) Data in (E) were normalized by pStat5 gMFI without treatment per mouse to calculate fold change. Nonlinear regression analysis with extra-sum-of-squares F test. $n = 3$ mice.

significant increase in overall CD4$^+$Foxp3$^+$ Treg percentage (12.50 ± 2.57%) compared with IGF1 or IAC alone (5.32 ± 0.77% or 6.83 ± 0.77%, respectively) or PBS control (3.54 ± 0.41) at 1 wk after the start of treatment (Fig. 3B, 3C). This resulted in a significant fold-increase in CD4$^+$Foxp3$^+$ Tregs from baseline in the IGF1 + IAC group (3.45 ± 0.46) compared with IAC and IGF1 treatment alone (1.89 ± 0.40 and 1.24 ± 0.19) (Fig. 3B, 3C). Treg expansion in the IGF1 + IAC group was due to proliferation of the Helios$^+$ thymically-derived Tregs (tTregs; IGF1 + IAC versus PBS: 9.67 ± 2.34% versus 2.02 ± 0.20%) rather than Helios$^-$ peripherally-induced Treg (pTreg) population (Fig. 3D, 3E) (39, 40). This was reflected by a significant fold-increase in tTregs, but not pTregs, in the combination treatment group (5.37 ± 0.60) as compared with the PBS (1.14 ± 0.21), IAC (2.74 ± 0.50), and IGF1 (1.61 ± 0.28) groups (Fig. 3D, 3E). Importantly, the observed increase in tTreg proportions occurred without off-target expansion of CD4$^+$ Foxp3$^-$ Tconvs, CD8$^+$ T cells, or NK cells (Fig. 4). Although the percentage of CD4$^+$Foxp3$^+$ Tregs remained increased in the IGF1 + IAC group at 2 wk posttreatment as compared with PBS control, the levels were already beginning to contract to those observed pretreatment and were no longer statistically different from other treatment groups by 3 wk posttreatment (Fig. 3B, 3C).

We further characterized the phenotype of Tregs that were expanded in peripheral blood at 1 wk posttreatment and observed significantly greater percentages of both CD44$^+$CD122$^+$ memory Tregs (IGF1 + IAC versus PBS: 7.98 ± 1.69% versus 2.28 ± 0.19%; Fig. 5A, 5B) and CD44$^-$CD122$^-$ naive Tregs (IGF1 + IAC versus PBS: 3.31 ± 0.81% versus 0.95 ± 0.24%; Fig. 5C, 5D). Likewise, both CD5^{hi} self-reactive Tregs (IGF1 + IAC versus PBS: 1.03 ± 0.26% versus 0.29 ± 0.03%; Fig. 5E, 5F) and CD5^{lo} polyclonal Tregs (IGF1 + IAC versus PBS: 2.00 ± 0.48% versus 0.54 ± 0.07%; Fig. 5G, 5H) were expanded by the combination treatment (41). Together, these data suggest that IGF1 + IAC treatment is likely to broadly impact Treg expansion in vivo. Similar to observations in peripheral blood (Fig. 3B, 3C), by 3 wk posttreatment, Treg percentages were not increased in the spleen (Fig. 6A, 6B) or pancreatic lymph nodes (pLNs) (Fig. 6C, 6D) of the IGF1 ± IAC groups. However, Treg functionality appeared to be enhanced in the IAC and IGF1 + IAC groups at 3 wk posttreatment, as evidenced by increased percentages of CD39$^+$CD73$^+$ Tregs, capable of converting ATP to immunosuppressive adenosine (42), in the spleen (IAC: 83.18 ± 1.85% and IGF1 + IAC: 83.70 ± 1.54% versus PBS: 77.80 ± 3.70%; Fig. 6E, 6F), lymph nodes (IAC: 71.65 ± 2.81% and IGF1 + IAC: 76.08 ± 1.84% versus PBS: 61.73 ± 5.20%;

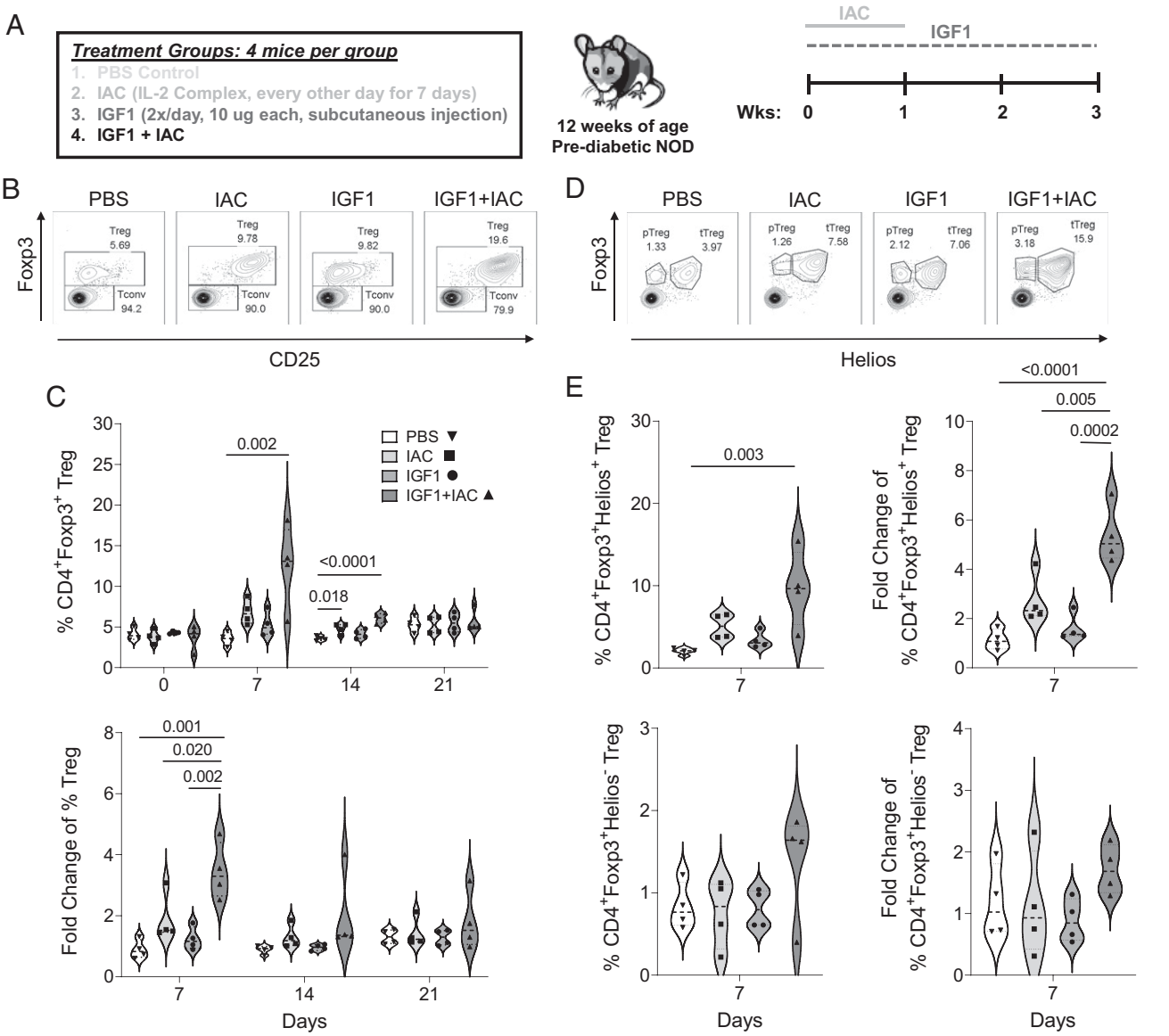

FIGURE 3. IGF1 treatment stimulates Tregs and synergizes with IL-2. (**A**) Experimental scheme. Prediabetic NOD mice were treated with PBS, IAC (anti–IL-2 [JES6.1] + recombinant mouse IL-2), IGF1, or IGF1 + IAC starting at 12 wk of age. IL-2 complex was delivered every other day for 7 d, whereas IGF-1 was delivered as 10 μg s.c. injections twice a day for a duration of 3 wk. Peripheral blood was collected for flow cytometric analysis before treatment and weekly for up to 3 wk posttreatment. (**B**) Representative contour plots showing $CD4^+Foxp3^+CD25^+$ Tregs and $CD4^+Foxp3^-$ Tconvs in peripheral blood after 1 wk of treatment. (**C**) Percentage of $CD4^+Foxp3^+CD25^+$ Tregs within $CD45^+CD19^-Ly6G^-$ cells at 0, 7, 14, and 21 d in PBS-, IAC-, IGF1-, and IGF1 + IAC-treated groups. One-way ANOVA with Dunnett's multiple comparison with the PBS time point. Fold change of Tregs over day 0 in the peripheral blood 1, 2, and 3 wk after the start of treatments. One-way ANOVA with Tukey's multiple comparison at each time point. (**D**) Representative contour plots showing Foxp3 and Helios expression on $CD4^+$ T cells in peripheral blood after 1 wk of treatment. (**E**) Percentage of $CD4^+Foxp3^+Helios^+$ tTregs and $CD4^+Foxp3^+Helios^-$ pTregs within $CD45^+CD19^-Ly6G^-$ cells. Fold change of tTregs and pTregs over day 0 in the peripheral blood at 1 wk after the start of treatments. One-way ANOVA with Tukey's multiple comparison. One-way ANOVA with Dunnett's multiple comparison with the PBS time point. $n = 4$ mice per group.

Fig. 6G, 6H), and thymi (IAC: 72.60 ± 3.12% and IGF1 + IAC: 66.70 ± 3.77% versus PBS: 61.28 ± 0.97%; Fig. 6I, 6J). These findings suggest that IGF1 and low-dose IL-2 independently induce an enduring capacity to perform a known mechanism of Treg suppression, while synergizing to transiently promote Treg-specific proliferation in vivo. These observations led us to test potential mechanisms behind this synergism.

IGF1 + IL-2 upregulates IL-2Rγ subunit expression in Tregs

We hypothesized that IL-2 + IGF1-mediated proliferation of Tregs might occur as a consequence of increased sensitivity to either factor via upregulation of their cognate receptors or subunits thereof. Thus, to elucidate the mechanism of IL-2 + IGF1 synergism, we assessed whether IGF1 modulates expression of any of the IL-2R subunits (IL-2Rα/CD25, IL-2Rβ/CD122, and IL-2Rγ/common γ-chain/CD132) or whether IL-2 modulates IGF1R expression by murine $CD4^+$ T cells. Although we observed that a short-term culture with the combination treatment of IL-2 and IGF1 did not enhance CD25 or CD122 expression on $Foxp3^+Helios^+$ Tregs as compared with IL-2 alone, IL-2 + IGF1 significantly increased CD132 expression versus IL-2 or IGF1 alone conditions (gMFI of 3001 ± 329 versus 2693 ± 314 or 2688 ± 314; Fig. 7A, 7B, Supplemental Fig. 1D). IGF1R expression on Tregs was not upregulated by the combination treatment as compared with IGF1 alone. Rather, IL-2 appeared to decrease IGF1R expression on Tregs (IL-2: 2883 ± 287 and IL-2 + IGF1: 2656 ± 409 versus no treatment: 4304 ± 263; Fig. 7A, 7B), in

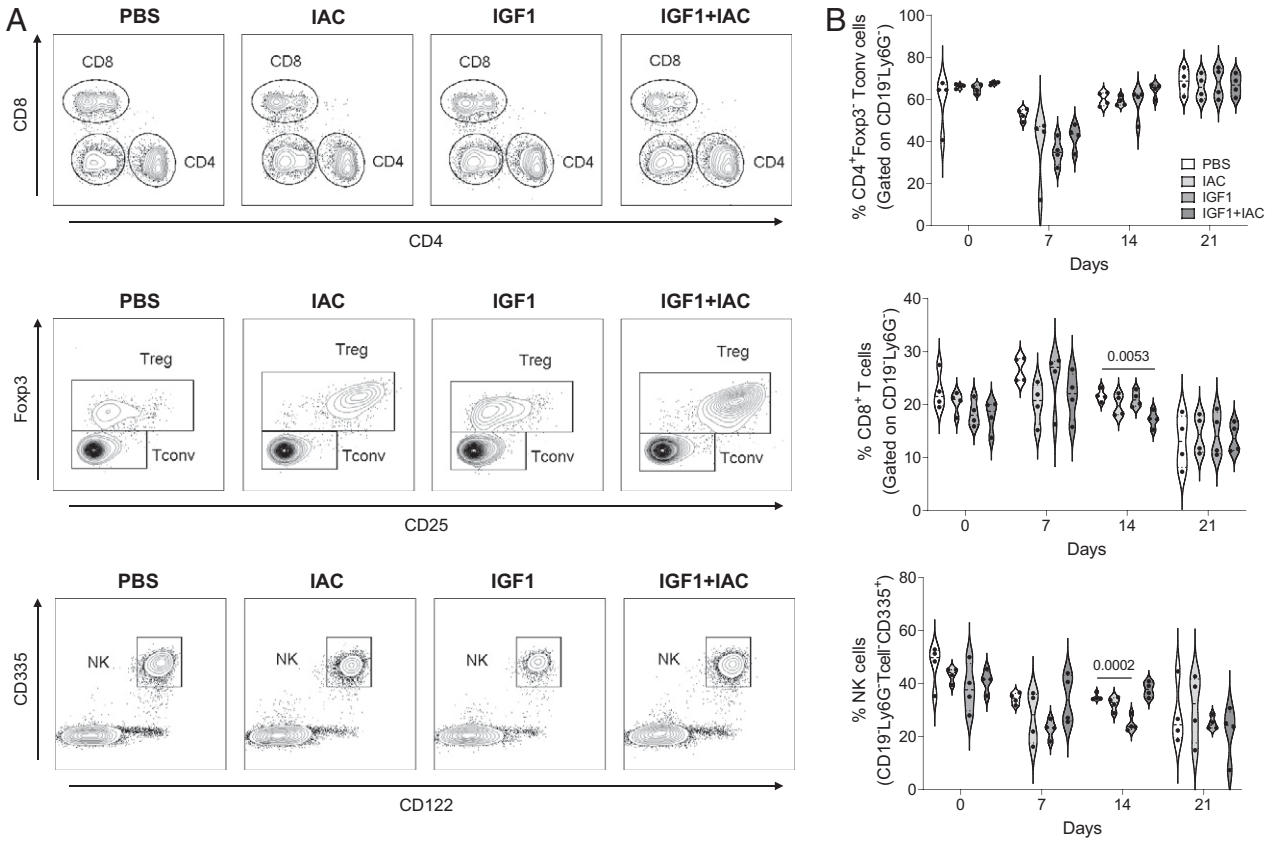

FIGURE 4. Off-target effects of IGF1 + IAC treatment in NOD mice. (**A**) Representative contour plots showing gating of $CD4^+Foxp3^-$ Tconvs and $CD8^+$ T cells (pregated on $CD19^-Ly6G^-$ cells), as well as $CD335^+CD122^+$ NK cells (pregated on $CD19^-Ly6G^-CD4^-CD8^-$ cells), in peripheral blood at 1 wk posttreatment. (**B**) Percentage of Tconvs, $CD8^+$ T cells, and NK cells at 0, 7, 14, and 21 d in mice treated with PBS, IAC, IGF1, or IGF1 + IAC. One-way ANOVA with Dunnett's multiple comparison with the PBS time point. $n = 4$ mice per group.

agreement with previous reports that IGF1R expression transiently decreases upon T cell activation (43, 44). Interestingly, IL-2 + IGF1 did not enhance IL-2R subunit expression beyond IL-2 alone or IGF1R expression beyond IGF1 alone on $CD62L^+CD44^-Foxp3^-Helios^-$ naive or $CD62L^-CD44^+Foxp3^-Helios^-$ memory Tconvs (Fig. 7C–F), suggesting that the synergistic effects of the combination treatment were limited to Tregs. Together, these findings imply that IL-2 + IGF1 promotes common γ-chain cytokine sensitivity in Tregs. These murine studies prompted us to assess the impact of the combination treatment on human Tregs.

Naive human Tregs express high levels of IGF1R

To understand whether differential IGF1R levels observed on T cell subsets from the T1D-prone NOD mouse may translate to human subjects, IGF1R (CD221) expression was quantified by flow cytometry on $CD4^+$ T cell subsets from fresh whole blood of children aged 4–16 y with and without T1D ($n = 14$ and $n = 15$, respectively; Table I). Analyzing the total cohort together, IGF1R expression was significantly higher on naive ($CD45RA^+CD197^+$) versus memory ($CD45RA^-$) $CD4^+$ T cells (Fig. 8A, 8B, Supplemental Fig. 2A), in agreement with previous reports from human studies (43) but in direct contrast with findings in mice (Fig. 1C, 1D, Supplemental Fig. 1B) (36). Intriguingly, naive Tregs ($CD45RA^+CD197^+CD25^{hi}CD127^{lo/-}$) showed significantly higher IGF1R expression than all other subsets assessed, including naive Tconvs ($CD45RA^+CD197^+CD127^+$) (Fig. 8A, 8B, Supplemental Fig. 2A), suggesting that naive Tregs may preferentially respond to IGF1 in humans.

IGF1R mRNA expression has previously been shown to decrease in human PBMCs with aging in adult subjects (45); however, immune subset-specific IGF1R expression has been poorly characterized. We observed that IGF1R levels displayed a significant negative correlation with subject age in a pediatric cohort in the naive Tconv ($R = -0.54$, $p = 0.003$; Fig. 8C) and naive Treg ($R = -0.58$, $p = 0.001$; Fig. 8D) compartments, and this association was weaker but still apparent in memory Tconv ($R = -0.33$, $p = 0.084$; Fig. 8C) and memory Treg ($R = -0.37$, $p = 0.047$; Fig. 8D) subsets. Collectively, our findings suggest that IGF1 may preferentially induce signaling in naive $CD4^+$ T cells, including naive Tregs, particularly in early life when T cell maturation remains active (46).

We also compared IGF1R expression on T cell subsets from subjects with and without T1D (Table I) to determine whether disease status might impact the degree of IGF1 signaling in $CD4^+$ T cells. In contrast with known modulation of peripheral IGF1 levels in T1D (22), IGF1R levels on naive Tconvs, memory Tconvs, naive Tregs, and memory Tregs were similar when comparing diabetes-free subjects with age- and sex-matched subjects with T1D (Fig. 8E). These data suggest that IGF1R expression on $CD4^+$ T cells is not impaired in T1D subjects.

IGF1 preferentially signals to human naive versus memory $CD4^+$ T cells

Observed differences in receptor expression suggest that IGF1 may preferentially induce IGF1R signaling in naive as compared with memory $CD4^+$ T cells, although to our knowledge, this question has yet to be formally experimentally tested. Therefore, we measured whether IGF1 preferentially augmented phosphorylation of PI3K/Akt pathway targets, downstream of IGF1R, in $CD4^+$ T cell subsets in the context of TCR stimulation (Table II). In this study, we observed that pAkt (Ser473) was enhanced by IGF1 treatment to a significantly greater extent in naive ($CD45RA^+$) than in memory ($CD45RA^-$) $CD4^+$ T cells at 15 min (1.17-fold difference) and 30 min (1.17-fold

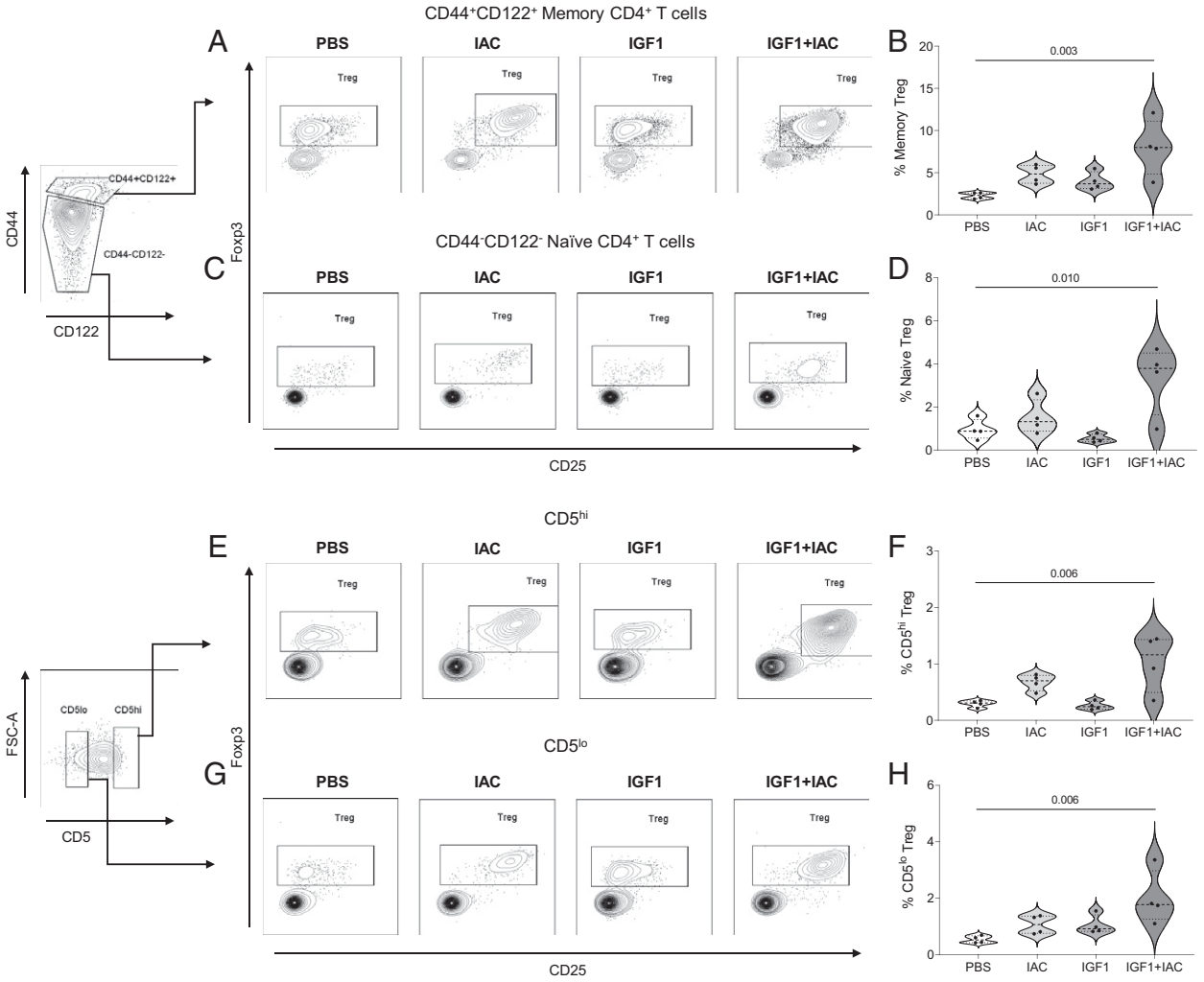

FIGURE 5. Treg subsets expanded in peripheral blood by 1 wk of IAC + IGF1 treatment. (**A**) Representative contour plots showing $CD25^+Foxp3^+$ Tregs within $CD44^+CD122^+$ memory $CD4^+$ T cells in PBS, IAC, IGF1, and IGF1 + IAC groups. (**B**) Percentage of memory Tregs within $CD45^+CD19^-Ly6G^-$ cells. (**C**) Representative contour plots showing $CD25^+Foxp3^+$ Tregs within $CD44^-CD122^-$ naive $CD4^+$ T cells in PBS, IAC, IGF1, and IGF1 + IAC groups. (**D**) Percentage of naive Tregs within $CD45^+CD19^-Ly6G^-$ cells. (**E**) Representative contour plots showing $CD25^+Foxp3^+$ Tregs within $CD5^{hi}$ $CD4^+$ T cells in PBS, IAC, IGF1, and IGF1 + IAC groups. (**F**) Percentage of $CD5^{hi}$ Tregs within $CD45^+CD19^-Ly6G^-$ cells. (**G**) Representative contour plots showing $CD25^+Foxp3^+$ Tregs within $CD5^{lo}CD4^+$ T cells in PBS, IAC, IGF1, and IGF1 + IAC groups. (**H**) Percentage of $CD5^{lo}$ Tregs within $CD45^+$ $CD19^-Ly6G^-$ cells. One-way ANOVA with Dunnett's multiple comparison with the PBS time point. $n = 4$ mice per group.

difference; Supplemental Fig. 3A, 3B). Likewise, downstream pS6 (Ser235/236) was upregulated by IGF1 to a greater extent in naive than in memory $CD4^+$ T cells at 15 min (1.23-fold difference) and 30 min (1.30-fold difference; Supplemental Fig. 3C, 3D). Although we observed that IGF1R expression was significantly higher on naive Tregs than naive Tconvs (Fig. 8A, 8B), naive $FOXP3^+Helios^+$ Tregs showed comparable IGF1R signaling induction to naive $FOXP3^-$ $Helios^-$ Tconvs (Supplemental Fig. 3E, 3F). These findings led us to question whether IGF1 would preferentially augment naive Treg proliferation if in the context of Treg-selective stimuli.

IGF1 augments IL-2–mediated homeostatic proliferation of naive human Tregs

Our observation of high IGF1R expression in naive Tregs implied that IGF1 could potentially synergize with IL-2 to preferentially induce the homeostatic proliferation of naive human Tregs in the absence of TCR stimulation (signal 1) or costimulation (signal 2). Thus, we treated bulk naive $CD4^+$ T cells with IL-2 and/or IGF1 to assess proliferation (Fig. 9A, Table II). Despite high levels of IGF1R on naive Tconvs (Fig. 8A, 8B), this subset did not proliferate in response to IGF1 stimulation ± supplementation with IL-2 (Fig. 9B). Although IGF1 alone was unable to induce the proliferation of naive $FOXP3^+Helios^+$ Tregs (Fig. 9B), the addition of IL-2 promoted the expansion of naive Tregs as compared with IL-2 alone (division index [DI]: 0.45 ± 0.21 versus 0.08 ± 0.11; Fig. 9B, 9C). Indeed, supplementation of low-dose IL-2 with IGF1 significantly increased the percentage of $FOXP3^+Helios^+$ Tregs within bulk naive $CD4^+$ T cell culture (4.74 ± 2.24% versus 3.09 ± 2.18%; Fig. 9D, 9E). Thus, IGF1 can synergize with low-dose IL-2 to specifically drive the homeostatic proliferation of naive Tregs.

IGF1 and γ-chain cytokines promote proliferation of transduced $CD4^+$ T cells while maintaining naivety

Maintenance of T cell naivety may prove beneficial in certain translational uses such as quiescent T cell expansion for autologous adoptive cellular therapies (47). In addition, the creation of Ag-specific T cell therapies for cancer or autoimmunity and the study of rare Ag-specific primary Treg and Tconv responses have been classically hindered by the need for activation to permit transduction with a receptor of interest (33, 34). Thus, we hypothesized that combinatorial IL-2 + IGF1 or IL-7 + IGF1 treatment would permit transduction of Tregs or Tconvs, respectively, while avoiding acquisition of a

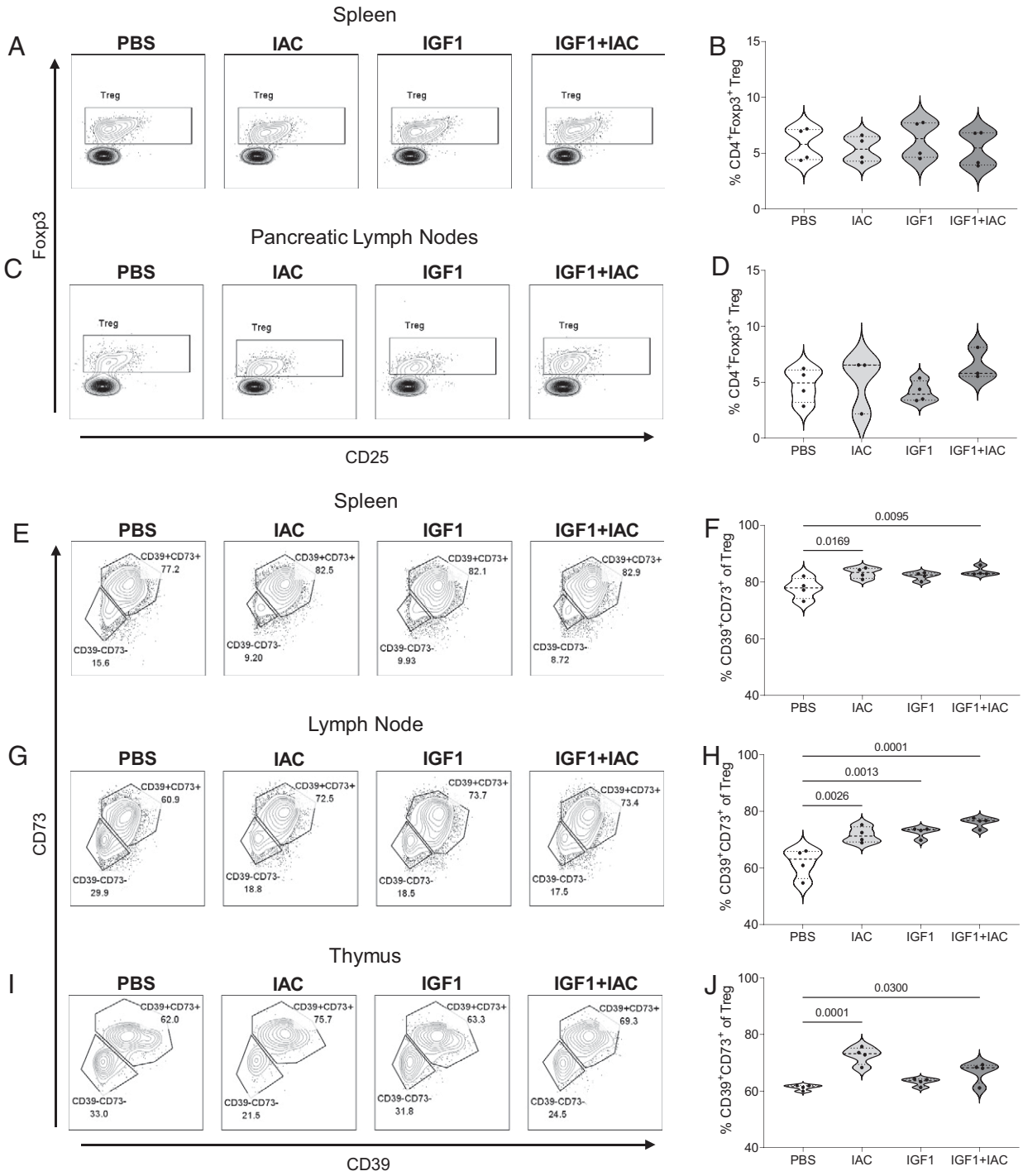

FIGURE 6. Increased $CD39^+CD73^+$ Tregs in lymphoid organs of IAC and/or IGF1-treated mice, despite similar Treg percentages at 3 wk posttreatment. (**A**) Representative contour plots showing $CD25^+Foxp3^+$ Treg gating within $CD4^+$ T cells of spleen at 21 d posttreatment in PBS, IAC, IGF1, and IGF1 + IAC groups. (**B**) Percentage of Tregs within $CD45^+CD19^-$ cells of spleen. (**C**) Representative contour plots showing $CD25^+Foxp3^+$ Treg gating within $CD4^+$ T cells of pLNs at 21 d posttreatment in PBS, IAC, IGF1, and IGF1 + IAC groups. (**D**) Percentage of Tregs within $CD45^+CD19^-$ cells of pLNs. (**E**) Representative contour plots showing CD39 and CD73 expression on Tregs of spleen at 21 d posttreatment in PBS, IAC, IGF1, and IGF1 + IAC groups. (**F**) Percentage of $CD39^+CD73^+$ cells within Tregs of spleen. (**G**) Representative contour plots showing CD39 and CD73 expression on Tregs of lymph nodes at 21 d posttreatment in PBS, IAC, IGF1, and IGF1 + IAC groups. (**H**) Percentage of $CD39^+CD73^+$ cells within Tregs of lymph nodes. (**I**) Representative contour plots showing CD39 and CD73 expression on Tregs of thymus at 21 d posttreatment in PBS, IAC, IGF1, and IGF1 + IAC groups. (**J**) Percentage of $CD39^+CD73^+$ cells within Tregs of thymus. One-way ANOVA with Dunnett's multiple comparison with the PBS time point. $n = 4$ mice per group.

memory phenotype. Indeed, pretreatment of naive $CD4^+$ T cells with IL-2 + IGF1, followed by transduction with a lentivirally encoded TCR recognizing the T1D-associated epitope GAD65 555–567 (32), significantly enhanced the proliferation of GAD65-reactive TRBV5-1^+ transduced naive Tregs beyond IL-2 alone (DI: 1.38 ± 0.91 versus 0.74 ± 0.69; Fig. 10A, 10B, Table II, Supplemental Fig. 2B). Similarly, IL-7 + IGF1 treatment significantly increased the DI of TRBV5-1^+ naive Tconvs as compared with IL-7 treatment alone (1.09 ± 0.52 versus 0.78 ± 0.55; Fig. 10A, 10B). Importantly, off-target proliferation of naive Tregs or naive Tconvs was not observed

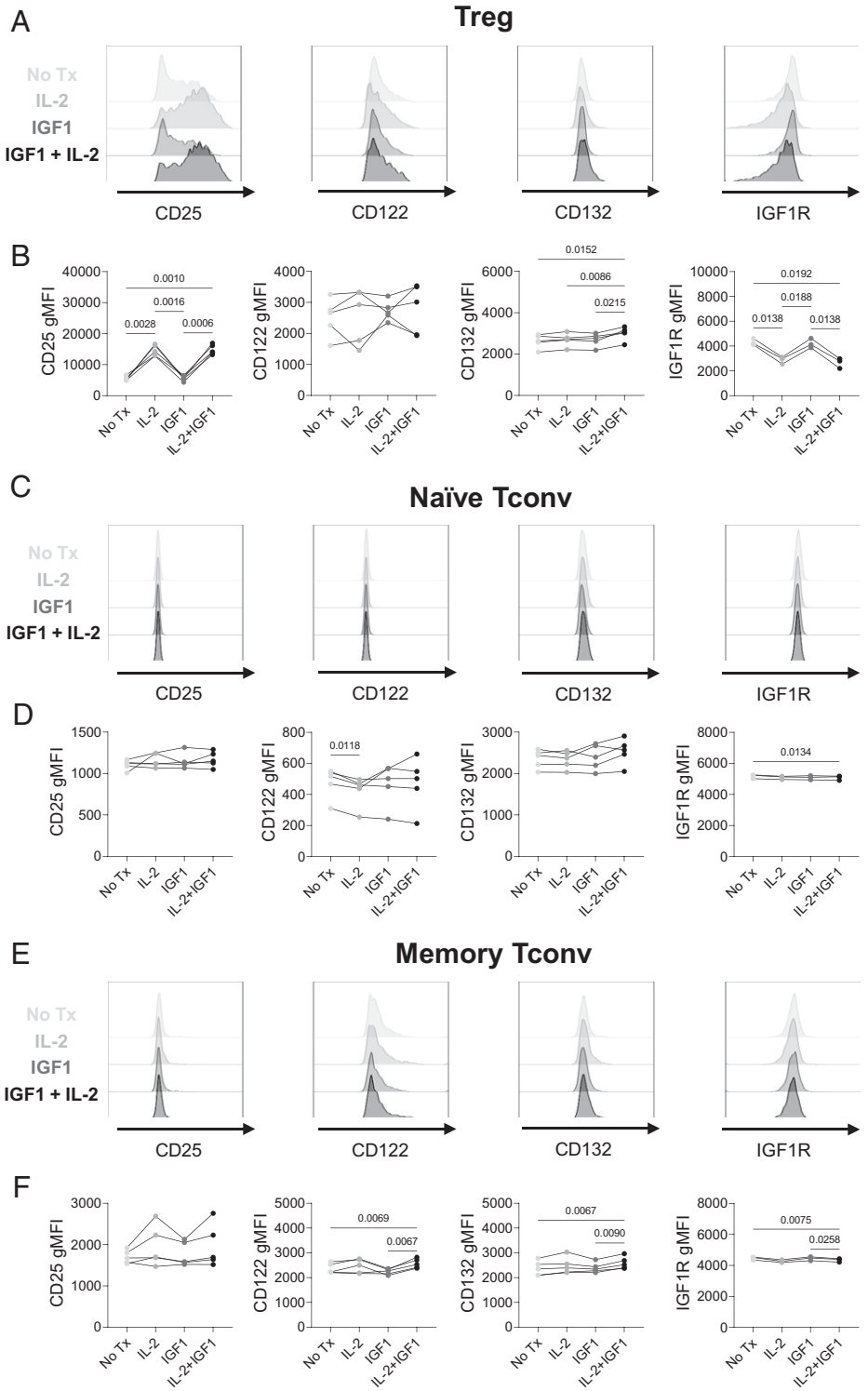

FIGURE 7. IGF1 + IL-2 modulates IL-2R subunit expression in Tregs. Splenocytes of 6- to 7-wk-old prediabetic mice were stimulated with 10 IU/ml rhIL-2, 100 ng/ml rhIGF1, IL-2 + IGF1, or neither (No Tx) for 2 d followed by flow cytometric staining for IL-2R subunits and IGF1R. (**A**) Representative histograms of CD25/IL-2Rα, CD122/IL-2Rβ, CD132/IL-2Rγ, and CD221/IGF1R expression on Tregs ($Foxp3^+Helios^+$). (**B**) gMFI of each marker on Tregs shown per mouse across treatment conditions. (**C**) Representative histograms of CD25/IL-2Rα, CD122/IL-2Rβ, CD132/IL-2Rγ, and CD221/IGF1R expression on naive Tconvs ($CD62L^+CD44^-Foxp3^-Helios^-$). (**D**) gMFI of each marker on naive Tconvs shown per mouse across treatment conditions. (**E**) Representative histograms of CD25/IL-2Rα, CD122/IL-2Rβ, CD132/IL-2Rγ, and CD221/IGF1R expression on memory Tconvs ($CD62L^-CD44^+Foxp3^-Helios^-$). (**F**) gMFI of each marker on memory Tconv shown per mouse across treatment conditions. Repeated-measures one-way ANOVA with Tukey's multiple comparisons test. $n = 5$ mice.

in the IL-7 ± IGF1 or IL-2 ± IGF1 conditions, respectively (Fig. 10A). Despite increased cell-type-specific proliferation, the overall transduction rate remained similar in IL-2 + IGF1 versus IL-2 and IL-7 + IGF1 versus IL-7 conditions (Fig. 10C, 10D). Importantly, Tregs and Tconvs expressing the lentivirally encoded T1D-associated TCR remained almost entirely $CD45RA^+CD197^+$ naive (Fig. 10E, 10F)

Table I. Demographic information for non-T1D and T1D subjects enrolled in whole blood IGF1R expression study

Cohort	Non-T1D	T1D
Total subjects, n	15	14
Sex, n (%)		
Male	7 (47)	7 (50)
Female	8 (53)	7 (50)
Age, y	12.3 ± 3.2	10.9 ± 2.8
Disease duration, y	N/A	3.0 ± 2.3

N/A, not applicable.

as opposed to traditional methods that generate mostly memory T cells (48, 49). Regarding functionality, enhanced Treg suppressive capacity has previously been shown to associate with higher levels of Foxp3 expression (50). Indeed, naive Treg FOXP3 gMFI was significantly increased in the IL-2 + IGF1 versus IL-2 alone condition (3947 ± 351 versus 3414 ± 239; Fig. 10G, 10H). Together, these data support a workflow where naive Ag-specific Tregs and Tconvs could be used to study primary activation events, which are of particular interest in conditions such as T1D wherein many genetic risk loci are tagged to regulators of T cell activation (51, 52).

Discussion

Although IL-2 is widely appreciated as an important regulator of Treg expansion and functional maintenance, the potential for off-target effects begs the question whether adjunctive treatments may synergize with and enable the use of low IL-2 doses. In this study, we sought to evaluate whether IGF1 augmented IL-2–mediated Treg expansion, initially characterizing patterns of IGF1R expression on T cell subsets. In agreement with our findings, previous studies support the notion that naive human $CD4^+$ T cells express significantly higher levels of IGF1R than memory $CD4^+$ T cells (43, 53), although this pattern is reversed in mice (36, 54). Despite this incongruity across species, we found novel evidence of naive human

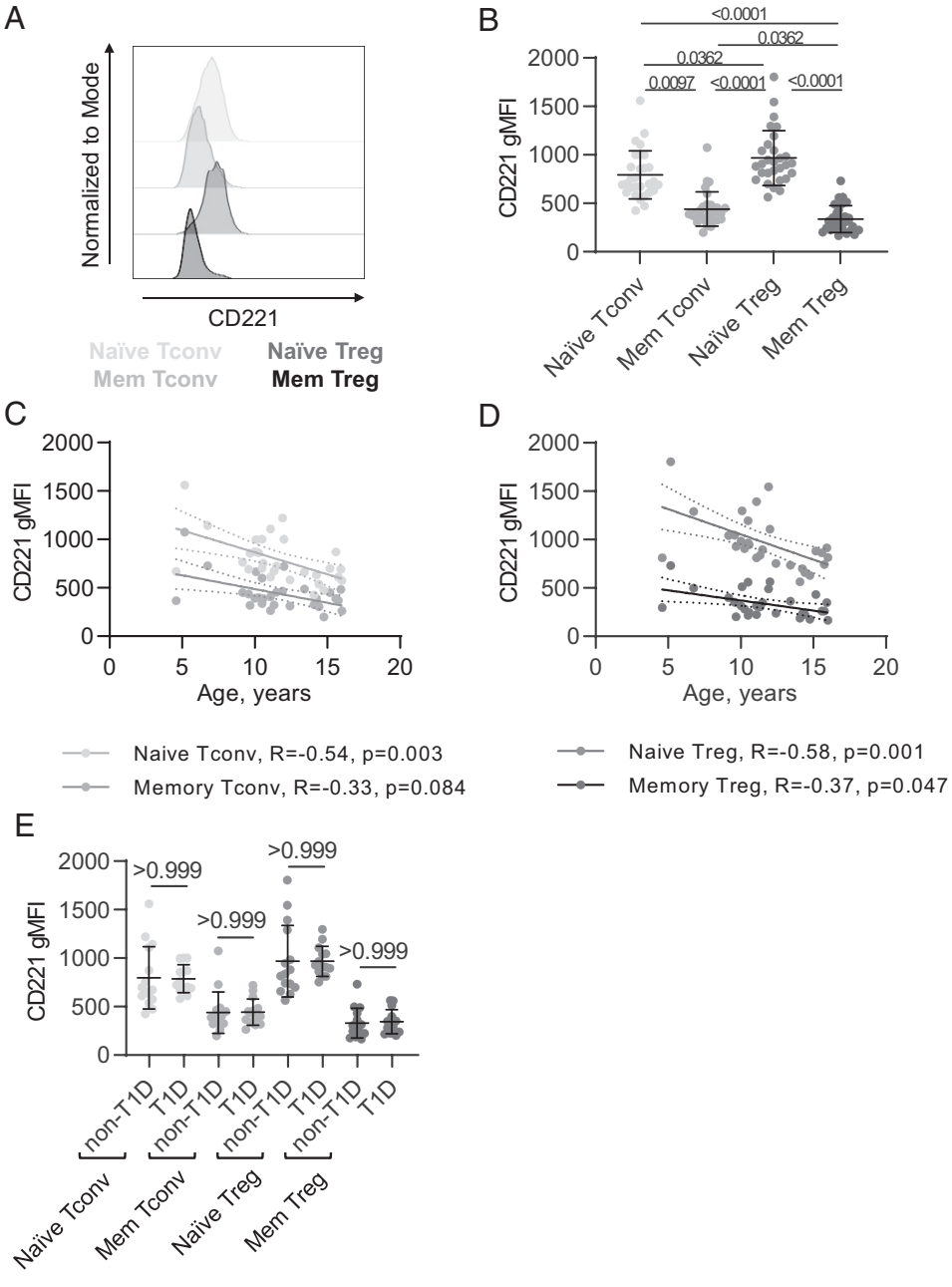

FIGURE 8. Naive human Tregs and Tconvs express significantly higher levels of IGF1R than memory Tregs and Tconvs. Whole blood staining was performed to further classify $CD3^+CD4^+$ T cells into naive ($CD45RA^+CD197^+$), memory ($CD45RA^-$), conventional ($CD127^+$), and regulatory ($CD25^{hi}CD127^{lo/-}$) subsets. (**A**) Representative histogram of gMFI of IGF1R (CD221) on naive Tregs, naive Tconvs, memory Tconvs, and memory Tregs within one subject. (**B**) IGF1R expression is highest on naive Tregs, followed closely by naive Tconvs. Memory Tconvs and memory Tregs show lowest IGF1R expression. Friedman test with Dunn's multiple comparisons test. Whole blood staining revealed a negative correlation between IGF1R gMFI and age of subject in years for (**C**) naive and memory Tconvs and (**D**) naive and memory Treg subsets. Best-fit third-order polynomial function shown (solid line) with 95% confidence intervals (dashed lines). Spearman correlation R and p values are shown below. (**E**) Comparison of CD221 gMFI on previously defined subsets between T1D and non-T1D subjects. Kruskal–Wallis test with Dunn's multiple comparisons test. $n = 29$ subjects.

Table II. Demographic information for subjects enrolled in IGF1R signaling, proliferation, and gene-editing studies

Cohort	Age, y	Sex
Signaling	5	F
	5	F
	12	M
	13	M
	22	F
	23	F
	26	M
	27	F
	29	F
Homeostatic proliferation	16	F
	18	M
	26	F
	41	F
	43	F
Gene editing	18	M
	20	F
	21	F
	22	F
	24	F

F, female; M, male.

Tregs expressing significantly elevated levels of IGF1R as compared with naive Tconv. This implies a potential role for IGF1 in maintaining the naive Treg pool. When taken together with our findings that younger human subject age and earlier murine thymocyte developmental stage are associated with increased IGF1R expression, these data suggest that IGF1 signaling may be important for naive Tregs in early development, with potential implications for modulating the survival or proliferation of Tregs at immature thymocyte stages (55).

Although IGF1 alone had a negligible impact on IGF1R signaling and Treg expansion, to our knowledge, we report the novel observation of IGF1 synergizing with IL-2 to enhance PI3K/Akt signaling in the absence of TCR ligation. This is in direct contrast with previous studies that have demonstrated induction of PI3K/Akt signaling upon IGF1 treatment of bulk primary human T cells (29, 56). However, these studies involved preactivation of T cells via TCR agonists (29, 56), suggesting that IGF1 may act as a regulator to amplify signaling pathways already engaged by T cells. Others have previously shown in vitro evidence of pS6 induction in murine Tregs by a truncated analogue of IGF1 (37) in addition to modest increases in pS6 by IL-2 (57), supporting our observation of IL-2 + IGF1 synergism in promoting Treg PI3K/Akt signaling. This enhancement of PI3K/Akt signaling implied that IL-2 + IGF1 may synergize to induce Treg proliferation.

Indeed, our studies show that IGF1 can specifically augment human tTreg proliferation in vitro and murine tTreg in vivo, in combination with low-dose IL-2. Others have previously shown that IGF1 alone can induce Treg skewing in human PBMCs (58, 59), although we did not observe an increase in pTreg induction in NOD mice, likely because of the discrepancy between IGF1R expression on naive T cells of mice and humans. Our work is unique in that it establishes the synergism of IGF1 with IL-2 and highlights the specificity of this treatment regimen for induction of naive human Treg proliferation. In contrast, in the murine in vivo treatment studies, expansions of both naive and memory, as well as $CD5^{hi}$ and $CD5^{lo}$, Tregs were observed. Future studies of TCR specificity will be required to understand whether the expanded $CD5^{hi}$ cells are bona fide autoreactive Tregs and to determine whether this translates to human Tregs as well. Regardless, consistent proliferation of the functionally stable tTreg population throughout our preclinical studies suggests that clinical studies may yield similar observations.

Furthermore, we observed that IL-2 + IGF1 upregulated expression of the intermediate-affinity IL-2R subunit, CD132, in murine Tregs to promote sensitivity to IL-2 and potentially other cytokines whose receptors use the common γ-chain. This is in contrast with a study in which culture with cellular supernatants containing IGF1 was shown to increase expression of the high-affinity IL-2R subunit, CD25, by induced human Tregs (58), although the authors did not test whether this could be directly attributed to the action of IGF1 or if this required other soluble factors. Thus, an important caveat of our work is that

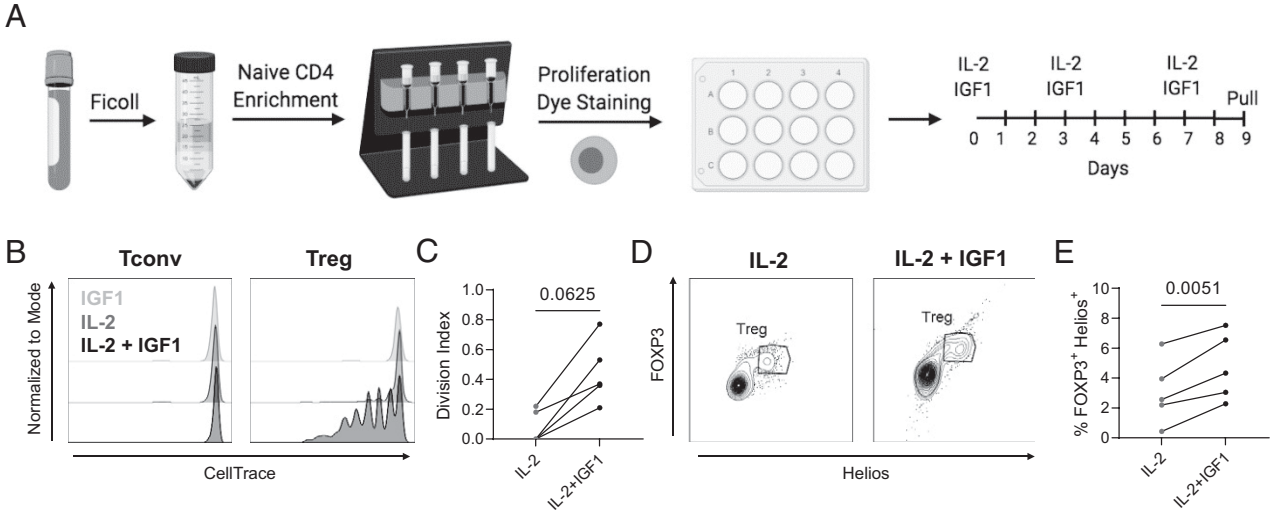

FIGURE 9. IGF1 augments the IL-2–mediated homeostatic proliferation of naive Tregs. (**A**) Methods for in vitro naive $CD4^+$ T cell homeostatic proliferation experiments. Density gradient centrifugation was performed to isolate PBMCs from whole blood, followed by magnetic bead–based naive $CD4^+$ T cell enrichment. Cells were stained with Cell Proliferation Dye eFluor670 to track proliferation before plating in complete RPMI supplemented with 20 IU/ml IL-2 and/or 100 ng/ml IGF1. Cytokines were replenished on days 3 and 7, and cultures were stained for flow cytometric analysis on days 9–11. Image created with BioRender. (**B**) Representative plots of cell proliferation dye in naive Tconvs and Tregs from IGF1, IL-2, and IL-2 + IGF1 conditions show (**C**) enhanced proliferation of naive Tregs in the presence of IL-2 + IGF1 versus IL-2 alone, as quantified by the DI. Wilcoxon test. (**D**) Representative plot of FOXP3 and Helios expression on $CD4^+CD45RA^+$ T cells showing that (**E**) percentage of $FOXP3^+Helios^+$ cells was increased upon treatment with IL-2 + IGF1 as compared with IL-2 alone. Paired *t* test. $n = 5$ subjects.

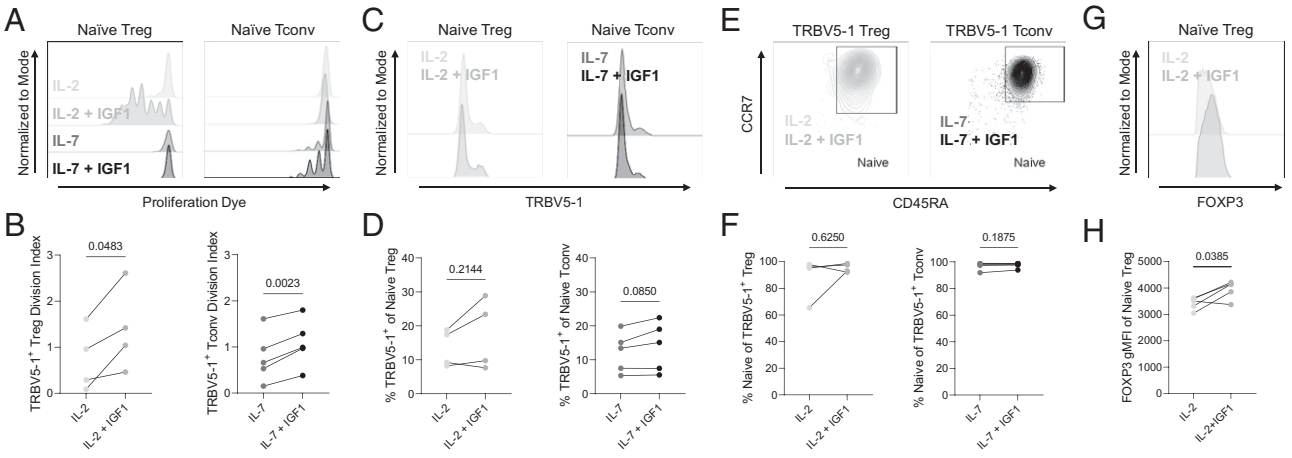

FIGURE 10. IGF1 and γ-chain cytokines promote proliferation of transduced $CD4^+$ T cells while maintaining naivety. Naive $CD4^+$ T cells were isolated and cultured with 20 IU/ml IL-2 or 10 ng/ml IL-7, with or without 100 ng/ml IGF1 for 7 d, followed by transduction with lentiviral constructs containing T1D-related β-cell–specific TCR R164, recognizing GAD 555–567 in the context of HLA-DRB1*04:01. (**A**) Seven days after transduction, dye dilution assay shows enhanced proliferation of naive transduced Tregs ($CD45RA^+CD197^+TRBV5\text{-}1^+FOXP3^+Helios^+$) with IL-2 + IGF1 as compared with IL-2 alone and enhanced proliferation of naive transduced Tconvs ($CD45RA^+CD197^+TRBV5\text{-}1^+FOXP3^-Helios^-$) with IL-7 + IGF1 versus IL-7 alone, (**B**) as quantified by DI. Paired *t* test. (**C**) Representative histograms of TRBV5-1 expression show similar transduction rates of naive Tregs with IL-2 versus IL-2 + IGF1 and naive Tconvs with IL-7 versus IL-7 + IGF1 treatment. (**D**) Percentage of $TRBV5\text{-}1^+$ cells transduced with R164 construct. Wilcoxon test. (**E**) Representative contour plots of CD45RA and CD197 expression on $TRBV5\text{-}1^+$ Tregs and Tconvs show transduced cells retain naivety. (**F**) Percentage of naive ($CD45RA^+CD197^+$) cells within the $TRBV5\text{-}1^+$ Treg and Tconv gates for IL-2 ± IGF1 and IL-7 ± IGF1 treatment, respectively. Paired *t* test. (**G**) Representative histograms of FOXP3 expression on naive Tregs. (**H**) FOXP3 gMFI on naive Tregs in IL-2 and IL-2 + IGF1 conditions. Paired *t* test. IL-2 ± IGF1, $n = 4$ subjects; IL-7 ± IGF1, $n = 5$ subjects.

that the influence of IGF1 on the inflammatory/regulatory balance may be highly dependent on the cytokine milieu.

Our observations of IGF1 potentially sensitizing Tregs to common γ-chain cytokine signaling inspired investigation into the application of IGF1 toward ex vivo homeostatic proliferation for gene transfer in primary human T cells. Others have previously shown successful transduction and maintenance of naivety in primary human $CD4^+$ and $CD8^+$ T cells by pretreating with IL-2 (60, 61) or IL-7 (60–62) without the use of conventional TCR activation stimuli, but this approach provides low cell yield, limiting their use in downstream experiments. In this study, we showed that the addition of IGF1 to IL-2 treatment not only enhanced the proliferation of transduced cells, but that this appeared to preferentially promote expansion of naive transduced Tregs. We also found that IGF1 augmented IL-7–mediated proliferation of transduced naive $CD4^+$ Tconvs, suggesting enhanced IL-7 signaling through CD132/IL-2Rγ (10). In addition to permitting the study of primary Ag-specific Treg and Tconv responses, of importance for in vitro modeling of autoimmunity and cancer (63), our combination treatment approach also has relevant clinical implications for autologous adoptive cellular therapies (47). Studies in the delivery of chimeric Ag receptor (CAR) T cells in cancer (64, 65) and CAR Tregs in inflammatory models (66) have clearly shown that therapeutic success is reliant on dampening of memory acquisition and hindering the development of cellular exhaustion. CAR Tregs, although proposed for treatment of autoimmunity, likewise require methodological fine-tuning for prevention of exhaustion and loss of lineage stability (67). Future studies should investigate whether the incorporation of IL-2 + IGF1 or IL-7 + IGF1 into CAR Treg or Tconv expansion protocols, respectively, prevents exhaustion to allow for longer duration of efficacy.

Our published work showing significantly lower peripheral IGF1 levels pre- and post-T1D (22) suggests that IGF1:IGF1R signaling may be impaired during disease development. Although IGF1R levels on $CD4^+$ T cells were comparable between healthy subjects and those with T1D, further studies of IGF1R expression pre-T1D may be necessary to rule out IGF1R dysregulation on $CD4^+$ T cells throughout the course of T1D pathogenesis. In combination with our observations in this study, decreased IGF1 signaling may contribute to autoimmunity (23) by inhibiting naive tTreg proliferation. However, an important caveat to this idea is that other groups have reported increased naive Tregs in the peripheral blood of children with T1D (68, 69), which could potentially reflect a decrease in this population at the site of autoimmunity. In line with this notion, targeted delivery methods for IL-2 + IGF1 treatment toward the pancreas and/or pLNs may need to be considered to rectify known Treg deficits in the pLNs in T1D (6, 70). Clearly, future efforts moving beyond peripheral blood to characterize immune phenotypes at the site of autoimmunity will be necessary to test these ideas, which remains a challenge in cases such as this where human and murine biology diverge. Regardless, future studies of pancreatic draining lymph nodes or pancreas in the IAC ± IGF1-treated mice may aid in elucidating how this therapy could impact diabetes pathogenesis.

In summary, we report that IGF1 augments naive human $CD4^+$ T cell sensitivity toward common γ-chain cytokines, and that this can be exploited via IGF1 + low-dose IL-2 treatment to drive the homeostatic proliferation of naive Tregs. We also present differences in murine and human IGF1R expression, highlighting the need for future studies of this pathway in human cells specifically. We believe our collective findings present a novel strategy toward rectifying the Treg/Tconv imbalance contributing to many autoimmune conditions. These data support additional studies to assess whether IGF1 can increase the IL-2–mediated homeostatic proliferation of naive Tregs in vivo or of autologous engineered Tregs ex vivo for translational benefit, representing potential strategies for clinical intervention to prevent or halt the progression of autoimmune disease, such as T1D.

Acknowledgments

We thank Kieran McGrail (UF) for technical assistance with biorepository management and procurement of demographic data and Rhonda Bacher (UF) for guidance on appropriate statistical methods. Special thanks are extended to all study subjects and their families for generously participating. We thank the clinical staff at UF, Nemours Children's Hospital, and Emory University for sample acquisition.

Disclosures

M.R.S. and T.M.B. are inventors on a patent filed by the UF, "Use of insulin-like growth factors with gamma-chain cytokines to induce homeostatic proliferation of lymphocytes," U.S. patent application serial no. 63/117,081.

References

1. Dejaco, C., C. Duftner, B. Grubeck-Loebenstein, and M. Schirmer. 2006. Imbalance of regulatory T cells in human autoimmune diseases. *Immunology* 117: 289–300.
2. Visperas, A., and D. A. Vignali. 2016. Are regulatory T cells defective in type 1 diabetes and can we fix them? *J. Immunol.* 197: 3762–3770.
3. Brusko, T., C. Wasserfall, K. McGrail, R. Schatz, H. L. Viener, D. Schatz, M. Haller, J. Rockell, P. Gottlieb, M. Clare-Salzler, and M. Atkinson. 2007. No alterations in the frequency of FOXP3+ regulatory T-cells in type 1 diabetes. *Diabetes* 56: 604–612.
4. Lindley, S., C. M. Dayan, A. Bishop, B. O. Roep, M. Peakman, and T. I. Tree. 2005. Defective suppressor function in CD4(+)CD25(+) T-cells from patients with type 1 diabetes. *Diabetes* 54: 92–99.
5. Putnam, A. L., F. Vendrame, F. Dotta, and P. A. Gottlieb. 2005. CD4+CD25high regulatory T cells in human autoimmune diabetes. *J. Autoimmun.* 24: 55–62.
6. Ferraro, A., C. Socci, A. Stabilini, A. Valle, P. Monti, L. Piemonti, R. Nano, S. Olek, P. Maffi, M. Scavini, et al. 2011. Expansion of Th17 cells and functional defects in T regulatory cells are key features of the pancreatic lymph nodes in patients with type 1 diabetes. *Diabetes* 60: 2903–2913.
7. Buckner, J. H. 2010. Mechanisms of impaired regulation by CD4(+)CD25(+)FOXP3(+) regulatory T cells in human autoimmune diseases. *Nat. Rev. Immunol.* 10: 849–859.
8. Dwyer, C. J., N. C. Ward, A. Pugliese, and T. R. Malek. 2016. Promoting immune regulation in type 1 diabetes using low-dose interleukin-2. *Curr. Diab. Rep.* 16: 46.
9. Liao, W., J. X. Lin, and W. J. Leonard. 2013. Interleukin-2 at the crossroads of effector responses, tolerance, and immunotherapy. *Immunity* 38: 13–25.
10. Lin, J. X., and W. J. Leonard. 2018. The common cytokine receptor γ chain family of cytokines. *Cold Spring Harb. Perspect. Biol.* 10: a028449.
11. Long, S. A., K. Cerosaletti, P. L. Bollyky, M. Tatum, H. Shilling, S. Zhang, Z. Y. Zhang, C. Pihoker, S. Sanda, C. Greenbaum, and J. H. Buckner. 2010. Defects in IL-2R signaling contribute to diminished maintenance of FOXP3 expression in CD4(+)CD25(+) regulatory T-cells of type 1 diabetic subjects. *Diabetes* 59: 407–415.
12. Long, S. A., K. Cerosaletti, J. Y. Wan, J. C. Ho, M. Tatum, S. Wei, H. G. Shilling, and J. H. Buckner. 2011. An autoimmune-associated variant in PTPN2 reveals an impairment of IL-2R signaling in CD4(+) T cells. *Genes Immun.* 12: 116–125.
13. Yang, J. H., A. J. Cutler, R. C. Ferreira, J. L. Reading, N. J. Cooper, C. Wallace, P. Clarke, D. J. Smyth, C. S. Boyce, G. J. Gao, et al. 2015. Natural variation in interleukin-2 sensitivity influences regulatory T-cell frequency and function in individuals with long-standing type 1 diabetes. *Diabetes* 64: 3891–3902.
14. Cerosaletti, K., A. Schneider, K. Schwedhelm, I. Frank, M. Tatum, S. Wei, E. Whalen, C. Greenbaum, M. Kita, J. Buckner, and S. A. Long. 2013. Multiple autoimmune-associated variants confer decreased IL-2R signaling in CD4+ CD25(hi) T cells of type 1 diabetic and multiple sclerosis patients. *PLoS One* 8: e83811.
15. Denny, P., C. J. Lord, N. J. Hill, J. V. Goy, E. R. Levy, P. L. Podolin, L. B. Peterson, L. S. Wicker, J. A. Todd, and P. A. Lyons. 1997. Mapping of the IDDM locus Idd3 to a 0.35-cM interval containing the interleukin-2 gene. *Diabetes* 46: 695–700.
16. James, C. R., I. Buckle, F. Muscate, M. Otsuka, M. Nakao, J. Sh. Oon, R. J. Steptoe, R. Thomas, and E. E. Hamilton-Williams. 2016. Reduced interleukin-2 responsiveness impairs the ability of Treg cells to compete for IL-2 in nonobese diabetic mice. *Immunol. Cell Biol.* 94: 509–519.
17. Tang, Q., J. Y. Adams, C. Penaranda, K. Melli, E. Piaggio, E. Sgouroudis, C. A. Piccirillo, B. L. Salomon, and J. A. Bluestone. 2008. Central role of defective interleukin-2 production in the triggering of islet autoimmune destruction. *Immunity* 28: 687–697.
18. Yu, A., I. Snowhite, F. Vendrame, M. Rosenzwajg, D. Klatzmann, A. Pugliese, and T. R. Malek. 2015. Selective IL-2 responsiveness of regulatory T cells through multiple intrinsic mechanisms supports the use of low-dose IL-2 therapy in type 1 diabetes. *Diabetes* 64: 2172–2183.
19. Boyman, O., M. Kovar, M. P. Rubinstein, C. D. Surh, and J. Sprent. 2006. Selective stimulation of T cell subsets with antibody-cytokine immune complexes. *Science* 311: 1924–1927.
20. Long, S. A., M. Rieck, S. Sanda, J. B. Bollyky, P. L. Samuels, R. Goland, A. Ahmann, A. Rabinovitch, S. Aggarwal, D. Phippard, et al.; Diabetes TrialNet and the Immune Tolerance Network. 2012. Rapamycin/IL-2 combination therapy in patients with type 1 diabetes augments Tregs yet transiently impairs β-cell function. *Diabetes* 61: 2340–2348.
21. Smith, T. J. 2010. Insulin-like growth factor-I regulation of immune function: a potential therapeutic target in autoimmune diseases? *Pharmacol. Rev.* 62: 199–236.
22. Shapiro, M. R., C. H. Wasserfall, S. M. McGrail, A. L. Posgai, R. Bacher, A. Muir, M. J. Haller, D. A. Schatz, J. D. Wesley, M. von Herrath, et al. 2020. Insulin-like growth factor dysregulation both preceding and following type 1 diabetes diagnosis. *Diabetes* 69: 413–423.
23. Shapiro, M. R., M. A. Atkinson, and T. M. Brusko. 2019. Pleiotropic roles of the insulin-like growth factor axis in type 1 diabetes. *Curr. Opin. Endocrinol. Diabetes Obes.* 26: 188–194.
24. Matsumoto, T., and T. Tsurumoto. 2002. Inappropriate serum levels of IGF-I and IGFBP-3 in patients with rheumatoid arthritis. *Rheumatology (Oxford)* 41: 352–353.
25. Thomas, A. G., J. M. Holly, F. Taylor, and V. Miller. 1993. Insulin like growth factor-I, insulin like growth factor binding protein-1, and insulin in childhood Crohn's disease. *Gut* 34: 944–947.
26. Katsanos, K. H., A. Tsatsoulis, D. Christodoulou, A. Challa, A. Katsaraki, and E. V. Tsianos. 2001. Reduced serum insulin-like growth factor-1 (IGF-1) and IGF-binding protein-3 levels in adults with inflammatory bowel disease. *Growth Horm. IGF Res.* 11: 364–367.
27. Bilbao, D., L. Luciani, B. Johannesson, A. Piszczek, and N. Rosenthal. 2014. Insulin-like growth factor-1 stimulates regulatory T cells and suppresses autoimmune disease. *EMBO Mol. Med.* 6: 1423–1435.
28. Johannesson, B., S. Sattler, E. Semenova, S. Pastore, T. M. Kennedy-Lydon, R. D. Sampson, M. D. Schneider, N. Rosenthal, and D. Bilbao. 2014. Insulin-like growth factor-1 induces regulatory T cell-mediated suppression of allergic contact dermatitis in mice. *Dis. Model. Mech.* 7: 977–985.
29. Mirdamadi, Y., U. Bommhardt, A. Goihl, K. Guttek, C. C. Zouboulis, S. Quist, and H. Gollnick. 2017. Insulin and insulin-like growth factor-1 can activate the phosphoinositide-3-kinase /Akt/FoxO1 pathway in T cells *in vitro*. *Dermatoendocrinol* 9: e1356518.
30. Cabello-Kindelan, C., S. Mackey, A. Sands, J. Rodriguez, C. Vazquez, A. Pugliese, and A. L. Bayer. 2020. Immunomodulation followed by antigen-specific T_{reg} infusion controls islet autoimmunity. *Diabetes* 69: 215–227.
31. Bergerot, I., N. Fabien, V. Maguer, and C. Thivolet. 1995. Insulin-like growth factor-1 (IGF-1) protects NOD mice from insulitis and diabetes. *Clin. Exp. Immunol.* 102: 335–340.
32. Reijonen, H., R. Mallone, A. K. Heninger, E. M. Laughlin, S. A. Kochik, B. Falk, W. W. Kwok, C. Greenbaum, and G. T. Nepom. 2004. GAD65-specific CD4+ T-cells with high antigen avidity are prevalent in peripheral blood of patients with type 1 diabetes. *Diabetes* 53: 1987–1994.
33. Yeh, W. I., H. R. Seay, B. Newby, A. L. Posgai, F. B. Moniz, A. Michels, C. E. Mathews, J. A. Bluestone, and T. M. Brusko. 2017. Avidity and bystander suppressive capacity of human regulatory t cells expressing *de novo* autoreactive T-cell receptors in type 1 diabetes. *Front. Immunol.* 8: 1313.
34. Brusko, T. M., R. C. Koya, S. Zhu, M. R. Lee, A. L. Putnam, S. A. McClymont, M. I. Nishimura, S. Han, L. J. Chang, M. A. Atkinson, et al. 2010. Human antigen-specific regulatory T cells generated by T cell receptor gene transfer. *PLoS One* 5: e11726.
35. Kooijman, R., L. E. Scholtens, G. T. Rijkers, and B. J. Zegers. 1995. Type I insulin-like growth factor receptor expression in different developmental stages of human thymocytes. *J. Endocrinol.* 147: 203–209.
36. Erlandsson, M. C., S. Töyrä Silfverswärd, M. Nadali, M. Turkkila, M. N. D. Svensson, I. M. Jonsson, K. M. E. Andersson, and M. I. Bokarewa. 2017. IGF-1R signalling contributes to IL-6 production and T cell dependent inflammation in rheumatoid arthritis. *Biochim. Biophys. Acta Mol. Basis Dis.* 1863: 2158–2170.
37. DiToro, D., S. N. Harbour, J. K. Bando, G. Benavides, S. Witte, V. A. Laufer, C. Moseley, J. R. Singer, B. Frey, H. Turner, et al. 2020. Insulin-like growth factors are key regulators of t helper 17 regulatory T cell balance in autoimmunity. *Immunity* 52: 650–667.e10.
38. Silva, S. L., A. S. Albuquerque, A. Serra-Caetano, R. B. Foxall, A. R. Pires, P. Matoso, S. M. Fernandes, J. Ferreira, R. Cheynier, R. M. Victorino, et al. 2016. Human naïve regulatory T-cells feature high steady-state turnover and are maintained by IL-7. *Oncotarget* 7: 12163–12175.
39. Thornton, A. M., P. E. Korty, D. Q. Tran, E. A. Wohlfert, P. E. Murray, Y. Belkaid, and E. M. Shevach. 2010. Expression of Helios, an Ikaros transcription factor family member, differentiates thymic-derived from peripherally induced Foxp3+ T regulatory cells. *J. Immunol.* 184: 3433–3441.
40. Thornton, A. M., and E. M. Shevach. 2019. Helios: still behind the clouds. *Immunology* 158: 161–170.
41. Sprouse, M. L., M. A. Scavuzzo, S. Blum, I. Shevchenko, T. Lee, G. Makedonas, M. Borowiak, M. L. Bettini, and M. Bettini. 2018. High self-reactivity drives T-bet and potentiates Treg function in tissue-specific autoimmunity. *JCI Insight* 3: e97322.
42. Deaglio, S., K. M. Dwyer, W. Gao, D. Friedman, A. Usheva, A. Erat, J. F. Chen, K. Enjyoji, J. Linden, M. Oukka, et al. 2007. Adenosine generation catalyzed by CD39 and CD73 expressed on regulatory T cells mediates immune suppression. *J. Exp. Med.* 204: 1257–1265.
43. Kooijman, R. K., L. E. Scholtens, G. T. Rijkers, and B. J. Zegers. 1995. Differential expression of type I insulin-like growth factor receptors in different stages of human T cells. *Eur. J. Immunol.* 25: 931–935.
44. Schillaci, R., M. G. Brocardo, A. Galeano, and A. Roldán. 1998. Downregulation of insulin-like growth factor-1 receptor (IGF-1R) expression in human T lymphocyte activation. *Cell. Immunol.* 183: 157–161.
45. Budzinska, M., M. Owczarz, E. Pawlik-Pachucka, M. Roszkowska-Gancarz, P. Slusarczyk, and M. Puzianowska-Kuznicka. 2016. miR-96, miR-145 and miR-9 expression increases, and IGF-1R and FOXO1 expression decreases in peripheral blood mononuclear cells of aging humans. *BMC Geriatr.* 16: 200.
46. Palmer, D. B. 2013. The effect of age on thymic function. *Front. Immunol.* 4: 316.
47. Marshall II, G. P., J. Cserny, D. J. Perry, W. I. Yeh, H. R. Seay, A. G. Elsayed, A. L. Posgai, and T. M. Brusko. 2018. Clinical applications of regulatory T cells in adoptive cell therapies. *Cell Gene Ther. Insights* 4: 405–429.
48. Seay, H. R., A. L. Putnam, J. Cserny, A. L. Posgai, E. H. Rosenau, J. R. Wingard, K. F. Girard, M. Kraus, A. P. Lares, H. L. Brown, et al. 2016. Expansion of human Tregs from cryopreserved umbilical cord blood for GMP-compliant autologous adoptive cell transfer therapy. *Mol. Ther. Methods Clin. Dev.* 4: 178–191.
49. Bluestone, J. A., J. H. Buckner, M. Fitch, S. E. Gitelman, S. Gupta, M. K. Hellerstein, K. C. Herold, A. Lares, M. R. Lee, K. Li, et al. 2015. Type 1 diabetes immunotherapy using polyclonal regulatory T cells. *Sci. Transl. Med.* 7: 315ra189.

50. Chauhan, S. K., D. R. Saban, H. K. Lee, and R. Dana. 2009. Levels of Foxp3 in regulatory T cells reflect their functional status in transplantation. *J. Immunol.* 182: 148–153.
51. Shapiro, M. R., P. Thirawatananond, L. Peters, R. C. Sharp, S. Ogundare, A. L. Posgai, D. J. Perry, and T. M. Brusko. 2021. De-coding genetic risk variants in type 1 diabetes. *Immunol. Cell Biol.* 99: 496–508.
52. Robertson, C. C., J. R. J. Inshaw, S. Onengut-Gumuscu, W. M. Chen, D. F. Santa Cruz, H. Yang, A. J. Cutler, D. J. M. Crouch, E. Farber, S. L. Bridges, Jr., et al.; Type 1 Diabetes Genetics Consortium. 2021. Fine-mapping, trans-ancestral and genomic analyses identify causal variants, cells, genes and drug targets for type 1 diabetes. *Nat. Genet.* 53: 962–971.
53. Douglas, R. S., A. G. Gianoukakis, S. Kamat, and T. J. Smith. 2007. Aberrant expression of the insulin-like growth factor-1 receptor by T cells from patients with Graves' disease may carry functional consequences for disease pathogenesis. *J. Immunol.* 178: 3281–3287.
54. Shay, T., V. Jojic, O. Zuk, K. Rothamel, D. Puyraimond-Zemmour, T. Feng, E. Wakamatsu, C. Benoist, D. Koller, A. Regev; ImmGen Consortium. 2013. Conservation and divergence in the transcriptional programs of the human and mouse immune systems. *Proc. Natl. Acad. Sci. USA* 110: 2946–2951.
55. Kecha, O., F. Brilot, H. Martens, N. Franchimont, C. Renard, R. Greimers, M. P. Defresne, R. Winkler, and V. Geenen. 2000. Involvement of insulin-like growth factors in early T cell development: a study using fetal thymic organ cultures. *Endocrinology* 141: 1209–1217.
56. Walsh, P. T., L. M. Smith, and R. O'Connor. 2002. Insulin-like growth factor-1 activates Akt and Jun N-terminal kinases (JNKs) in promoting the survival of T lymphocytes. *Immunology* 107: 461–471.
57. Yu, A., L. Zhu, N. H. Altman, and T. R. Malek. 2009. A low interleukin-2 receptor signaling threshold supports the development and homeostasis of T regulatory cells. *Immunity* 30: 204–217.
58. Miyagawa, I., S. Nakayamada, K. Nakano, K. Yamagata, K. Sakata, K. Yamaoka, and Y. Tanaka. 2017. Induction of regulatory T cells and its regulation with insulin-like growth factor/insulin-like growth factor binding protein-4 by human mesenchymal stem cells. *J. Immunol.* 199: 1616–1625.
59. Kimura, K., H. Hohjoh, M. Fukuoka, W. Sato, S. Oki, C. Tomi, H. Yamaguchi, T. Kondo, R. Takahashi, and T. Yamamura. 2018. Circulating exosomes suppress the induction of regulatory T cells via let-7i in multiple sclerosis. *Nat. Commun.* 9: 17.
60. Cavalieri, S., S. Cazzaniga, M. Geuna, Z. Magnani, C. Bordignon, L. Naldini, and C. Bonini. 2003. Human T lymphocytes transduced by lentiviral vectors in the absence of TCR activation maintain an intact immune competence. *Blood* 102: 497–505.
61. Unutmaz, D., V. N. KewalRamani, S. Marmon, and D. R. Littman. 1999. Cytokine signals are sufficient for HIV-1 infection of resting human T lymphocytes. *J. Exp. Med.* 189: 1735–1746.
62. Wang, S. Y., T. V. Moore, A. V. Dalheim, G. M. Scurti, and M. I. Nishimura. 2021. Melanoma reactive TCR-modified T cells generated without activation retain a less differentiated phenotype and mediate a superior in vivo response. *Sci. Rep.* 11: 13327.
63. Armitage, L. H., S. E. Stimpson, K. E. Santostefano, L. Sui, S. Ogundare, B. N. Newby, R. Castro-Gutierrez, M. K. Huber, J. P. Taylor, P. Sharma, et al. 2021. Use of induced pluripotent stem cells to build isogenic systems and investigate type 1 diabetes. *Front. Endocrinol. (Lausanne)* 12: 737276.
64. Zebley, C. C., C. Brown, T. Mi, Y. Fan, S. Alli, S. Boi, G. Galletti, E. Lugli, D. Langfitt, J. Y. Metais, et al. 2021. CD19-CAR T cells undergo exhaustion DNA methylation programming in patients with acute lymphoblastic leukemia. *Cell Rep.* 37: 110079.
65. Prinzing, B., C. C. Zebley, C. T. Petersen, Y. Fan, A. A. Anido, Z. Yi, P. Nguyen, H. Houke, M. Bell, D. Haydar, et al. 2021. Deleting DNMT3A in CAR T cells prevents exhaustion and enhances antitumor activity. *Sci. Transl. Med.* 13: eabh0272.
66. Rana, J., D. J. Perry, S. R. P. Kumar, M. Muñoz-Melero, R. Saboungi, T. M. Brusko, and M. Biswas. 2021. CAR- and TRuC-redirected regulatory T cells differ in capacity to control adaptive immunity to FVIII. *Mol. Ther.* 29: 2660–2676.
67. Lamarthée, B., A. Marchal, S. Charbonnier, T. Blein, J. Leon, E. Martin, L. Rabaux, K. Vogt, M. Titeux, M. Delville, et al. 2021. Transient mTOR inhibition rescues 4-1BB CAR-Tregs from tonic signal-induced dysfunction. *Nat. Commun.* 12: 6446.
68. Viisanen, T., A. M. Gazali, E. L. Ihantola, I. Ekman, K. Näntö-Salonen, R. Veijola, J. Toppari, M. Knip, J. Ilonen, and T. Kinnunen. 2019. FOXP3+ regulatory T cell compartment is altered in children with newly diagnosed type 1 diabetes but not in autoantibody-positive at-risk children. *Front. Immunol.* 10: 19.
69. Okubo, Y., H. Torrey, J. Butterworth, H. Zheng, and D. L. Faustman. 2016. Treg activation defect in type 1 diabetes: correction with TNFR2 agonism. *Clin. Transl. Immunology* 5: e56.
70. Sebastiani, G., G. Ventriglia, A. Stabilini, C. Socci, C. Morsiani, A. Laurenzi, L. Nigi, C. Formichi, B. Mfarrej, A. Petrelli, et al. 2017. Regulatory T-cells from pancreatic lymphnodes of patients with type-1 diabetes express increased levels of microRNA miR-125a-5p that limits CCR2 expression. *Sci. Rep.* 7: 6897.